EXPERIMENTAL AND FINITE ELEMENT STUDY OF THE DESIGN PARAMETERS OF AN ALUMINUM BASEBALL BAT

BY

GAYATRI VEDULA
B.TECH, JAWAHARLAL NEHRU TECHNOLOGICAL UNIVERSITY (2001)

SUBMITTED IN PARTIAL FULLFILMENT OF THE REQUIREMENTS FOR THE DEGREE OF MASTER OF SCIENCE IN MECHANICAL ENGINEEERING
DEPARTMENT OF MECHANICAL ENGINEERING
UNIVERSITY OF MASSACHUSETTS LOWELL

Signature of
Author: _____ Date: _____

Signature of Thesis
Supervisor: _____

Signatures of Other
Committee Members: _____

_____

EXPERIMENTAL AND FINITE ELEMENT STUDY OF THE DESIGN PARAMETERS OF AN ALUMINUM BASEBALL BAT

BY

GAYATRI VEDULA

ABSTRACT OF A THESIS SUBMITTED TO THE FACULTY OF THE
DEPARTMENT OF MECHANICAL ENGINEERING
IN PARTIAL FULLFILMENT OF THE REQUIREMENTS FOR THE DEGREE OF
MASTER OF SCIENCE IN MECHANICAL ENGINEEERING
DEPARTMENT OF MECHANICAL ENGINEERING
UNIVERSITY OF MASSACHUSETTS LOWELL
2004

Thesis Supervisor: James A Sherwood, PhD, P.E.
Professor, Department of Mechanical Engineering

ABSTRACT

In 1974, the NCAA introduced metal bats into collegiate-level baseball as a cost-effective alternative to traditional wood bats. Manufacturers of bats can change very little in the case of wood bats other than the outside profile because the properties of the wood are at the mercy of Mother Nature. In contrast, innovative methods of manufacturing and new alloys enable the design of metal bats that can have a wide range of performance. Players, fans and scientists are concerned that high-performance metal bats might compromise the integrity of the game. In this context, the goal of the current research is to study the different factors that affect the performance of metal and wood bats, as it may be useful to understand what physical properties influence the differences in the performance between wood and metal bats.

For this research, a metal bat and a wood bat are used. The mass, center of gravity, moment of inertia, center of percussion, sweet spot, batted-ball speed, fundamental frequencies and node points on one wood and one metal bat are measured experimentally. Finite element models of these two bats are then built, compared to experimental data, and calibrated with the experimental values. A parametric study of these finite element models is then done to understand the effect of various physical properties on the performance of the bats.

ACKNOWLEDGEMENTS

I would like to acknowledge the following individuals for supporting me through my master's and also in this research.

I would like to convey my sincere thanks to **Prof. James Sherwood,** my advisor and thesis supervisor for his support and suggestions throughout this research. His support and remarks have been very instrumental in bringing this research to a good shape. Also, I am thankful to **Prof. Peter Avitabile** for spending so much time with me and giving me valuable suggestions during the course of my thesis. I am thankful to **Prof. Sammy Shina** for being my committee member and giving me his comments.

I am thankful to **Prof. Alan Nathan** for his support and interest in my work. Thanks to **Tim Mustone,** for initiating this thesis and for helping with his suggestions whenever necessary. Also thanks to **Patrick Drane**, **Shintaro Nabeshima** and all the baseball students who helped in this process. Also thanks to **Jennifer Gorczyca**, **Samira Farboodmanesh**, **Kari White**, **Lu Liu, Xiang Li and Hiromuchi Tsuji** for their help and encouragement.

I would also like to thank my aunt **Mohini.N.Sastry** and uncle **N.S.Sastry** for helping financially and giving me accommodation during my master's. I also thank my parents, sister, Satish, Sravanthi and all other family members for their support and trust in me.

TABLE OF CONTENTS

LIST OF FIGURES

LIST OF TABLES

1 INTRODUCTION

In any field, technology always strives to provide a solution to an existing problem or a better solution to a previously addressed situation. This desire to progress and excel has led to many great inventions and discoveries. With the same intentions in 1974, the NCAA introduced metal bats as a cost-effective alternative to traditional wood bats. Initially, the wood and aluminum bats were considered to perform similarly. However, with the new technology and innovative methods of developing high-performance alloys, there was a concern about the increase in performance of metal bats. Even though advances in the technology are appreciated by the batters, baseball purists and scientists preach that any bat-performance increase will compromise the integrity of the game. The integrity of a game like baseball is preserved only if the outcome of the game is based on the players' skills and abilities and not because of technical advantages due to a material change in one of the essential tools of the game—the BAT.

In this context, studies conducted by Thurston [1] to evaluate the performance of metal bats show that the batting average of hitters was 0.331 with metal bats and 0.231 with wood bats. Based on his study (1997-2002), Thurston also concluded, "on average the ball comes off the metal bat 5.9 mph faster than off the wood bat '". Greenwald and Crisco [2] conducted a batting cage study with two wood bats and five metal bats to understand the differences in the performance. The pitch speeds and ball exit speeds were tracked using a commercially available system. The study revealed that metal bats do

outperform wood bats and the increase in performance was attributed to the trampoline effect and bat mass distribution. However, these results were limited to the test conditions, the bats and the players selected for the test. These studies paved the way for good research to further find out what causes a metal bat to perform better than wood–if it does at all.

1.1 MOTIVATION

Although, previous research (to be explained in Chapter 2) is available to understand some of the factors, a detailed study covering all the design parameters of metal bats is not available in the open literature. Complete knowledge of these design parameters and their effect on the performance of the bat is essential to understand what causes a change in the performance of a metal bat. The current research is an attempt to investigate the design parameters of a metal bat and a wood bat, using finite element analyses and experimental investigations.

Finite element analysis is a numerical procedure for analyzing structures and continua. With calibrated finite element models of the bat and ball, one can measure the contact time and calculate batted-ball speeds. The mode shapes of the bat can be animated so as to see how each mode is distributed along the length of the bat. Using finite element analysis makes it easy to change any parameter of the bat and the ball and see how the change affects the overall performance.

1.2 SCOPE

Ball exit velocities of wood and aluminum bats (33-inch long) tested at the University of Massachusetts Lowell Baseball Research Center (UMLBRC) were used in this research. Knowledge of previous research [3-5] was used to assist in identifying which factors effect the performance. For the current research, an aluminum bat that outperforms (experimentally found) a wood bat was chosen. The masses, moments of inertia, centers of gravity, frequencies, node points of the two fundamental modes, centers of percussion, and sweet spots of wood and aluminum bats were measured experimentally. Finite element models of the bats were then built using HyperMesh® [6] (for geometry and preprocessing). LS-DYNA© [7] was used for analysis and LS-Post and ETA Postprocessors were used for post-processing. The finite element models were compared and calibrated with the experimental values as applicable. A parametric study of these FE models was done to study what physical changes in the bat effect the performance (ball exit velocity) of the aluminum and wood bats.

2 NOMENCLATURE

The definitions and notations used in this thesis are defined in this section.

2.1 PERFORMANCE

The performance of the bat in this thesis always means ball exit velocity. A bat with a relatively high ball exit velocity is said to be high performing and vice versa.

2.2 SECTION OF BAT

The different sections of the bat referenced in this thesis are shown in Fig. 1. All measurements in this thesis are measured from the barrel end of the bat.

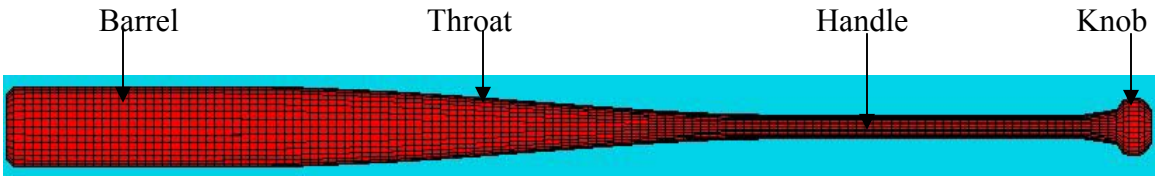

Fig. 1: Different sections of the bat

2.3 SWEET SPOT

The term sweet spot in this thesis refers to the impact location on the bat which produces maximum batted ball velocity. It is normally found 5 to 7 inches from the tip of the barrel of the bat.

2.4 Node 1

A node point is a location where the amplitude of vibration is zero. Node 1 in this thesis refers to the node of the first mode closest to the tip of the barrel of the bat.

2.5 Node 2

Node 2 refers to the node of the second mode closest to the tip of the barrel of the bat.

2.6 COP

Center of percussion is the impact location on the bat, which produces no sting or painful shock to the batter's hands.

2.7 Baum Hitting Machine (BHM)

The Baum hitting machine is a machine setup for standard baseball testing and swings a moving ball into a moving bat.

2.8 Hoop Mode or Breathing Mode

During collision, metal bat stores energy in the form of compression (strain energy) and this energy is restored to the ball. This type of breathing or compression and expansion mode of bat is known as the hoop mode or the breathing mode of the barrel and is sometimes also referred as the trampoline effect.

3 BACKGROUND

In this chapter, the basic theories used in the research and a discussion about the various factors affecting the performance of the bats are presented. Relevant previous research [3-5] is also included where available. Brief theoretical concepts related to Finite Element Analysis and Modal Analysis are also presented to familiarize the reader with these areas for the later chapters.

3.1 SWEET SPOT

The sweet spot has three interpretations. The sweet spot is commonly known as the location on the bat that produces maximum batted-ball velocity. Often, it is also understood as the location on the bat that produces no sting to the batter's hands. A third interpretation of the sweet spot is the location on the bat where the amplitude of fundamental vibrations is zero (node point). Physicists also think of the sweet spot as the optimal location on the bat that produces best overall results. However, in this thesis, the sweet spot is defined as the location on the bat that when impacted produces the highest ball exit velocity.

Experienced baseball players often feel that the best location to hit a ball lies about 5 to 7 inches from the tip of the barrel. The sweet spot [5] exists because it is close to the COP (center of percussion) and because the amplitude of fundamental vibrations at this location is minimal (close to node). The relationship amongst the sweet spot, the

COP and the node points is studied as part of this research in an effort to understand how each of these items influences the performance. Details about COP and node points are explained in the later sections in this chapter.

3.2 THEORY USED IN THE RESEARCH

Every sport is as much science as entertainment. In baseball, two bodies with different masses encounter each other at different velocities. Newton's second Law of motion can be used to explain a phenomenon like this:

Newton's second law of motion states, "The rate of change of momentum of an object is equal to the net force acting on it" (Eqn. 1) which is expressed as

$$\mathbf{F = dP / dt} \tag{1}$$

this force can be written for constant mass as,

$$\mathbf{F = m\ dv/dt} \tag{2}$$

where: F is force
P is the momentum
v is the velocity
m is the mass of the object under consideration

A baseball will travels towards the bat with an initial momentum $\boldsymbol{P}$ and the bat will be traveling towards the ball with an initial momentum $\boldsymbol{p}$. For the baseball to move in the opposite direction after contact there must be a momentum change. Newton's second law states that for a momentum change to occur, a force must be applied on the body. Now, over a short period of time (~0.001 s), the ball and the bat exert equal force on each other but in opposite directions. Because, in an isolated system, momentum is

conserved, and the initial momentum (bat + ball) must be equal to the final momentum. Therefore,

$$\mathbf{M}ball_{\mathbf{i}} * \mathbf{V}ball_{\mathbf{i}} + \mathbf{M}bat_{\mathbf{i}} * \mathbf{V}bat_{\mathbf{i}} = \mathbf{M}ball_{\mathbf{f}} * \mathbf{V}ball_{\mathbf{f}} + \mathbf{M}bat_{\mathbf{f}} * \mathbf{V}bat_{\mathbf{f}} \quad (3)$$

where: subscript *i* refers to the initial values
subscript *f* refers to final values
M is mass
V is velocity.

From Eqn. 3, it is inferred that the ball exit velocity is dependent on the initial velocities of the ball and the bat and their respective masses. Therefore, keeping the properties of the ball the same, the performance of the bat can be changed by altering either the mass or the initial velocity of the bat. In relation to the performance of the bat, it is found from previous research efforts [3-5] that the factors which affect the performance of a metal bat are mass, mass moment of inertia, center of gravity, wall thickness, center of percussion, sweet spot, fundamental frequencies, node points of fundamental vibration modes and the hoop-mode frequencies. Detailed descriptions of the effect of these factors on the performance of the bat are presented below.

3.2.1 Mass of the Bat

According to the NCAA standards for metal bats, the length to weight difference for metal bats (made after 1999) [8] should not exceed 3. That is, a 34-in. long bat should not weigh less than 31 oz. From, the conservation of momentum equation, it can be understood that increasing mass would bring increased momentum into collision and hence will increase ball exit velocity—assuming no change in swing speed due to the

increased mass. Therefore, the heavier the bat, the higher will be the ball exit velocity—implying high performance of the bat. However, as bat mass increases, swing speed decreases, and thus, the end result which is the increase in ball exit velocity may be compromised.

The influence of bat mass on the ball exit velocity can be understood from an experiment [9] in which the ball mass, pitch speed and bat swing speed were all kept constant and only the bat mass was changed. The mass of a bat weighing 20 oz. was doubled and the corresponding change in ball exit speed was measured. It was observed that the ball exit velocity then increased by 12 mph (from 68 to 80 mph). Hence, a heavier bat will produce higher ball exit velocity if the swing speed is kept constant.

3.2.2 Bat Swing Velocity

The bat swing velocity directly accounts for the initial momentum of the bat. Because momentum is given by the product of mass and velocity, relatively high initial velocity will give relatively high momentum. An experiment [9] conducted to understand the effect of bat swing velocity on the ball exit velocity gives some quantitative results in this context. In this experiment, the bat mass, ball mass and initial velocity were kept constant and only the bat swing speed was doubled (from 20.5 to 41.0 mph). The results from the experiment show that doubling the bat swing speed, results in an increase of 22 mph (from 62 to 84 mph) in the ball exit velocity. Therefore, doubling the bat swing speed has more effect on the ball exit velocity than doubling the mass of the bat (exit speed increased by 12 mph). The reason being, it is hard to swing a heavy bat at the same speed as a lightweight bat, therefore, the increase in mass might slightly compromise the

increase in initial momentum. Therefore, it is advantageous to swing the same bat at higher velocity than to swing a heavier bat at the same velocity.

3.2.3 Mass Moment of Inertia

The moment of inertia (MOI) by definition is the resistance to the angular acceleration of an object. The MOI of an object is a measure of the distribution of the mass along its length relative to an axis of rotation. The MOI is the product of mass and the square of the distance between the axis and the mass. In the case of a nonuniform object like a baseball bat, the MOI is the product of mass times the square of the distance to the mass summed over the entire length of the bat given as,

$$\mathbf{MOI} = \sum_i m_i r_i^2 = \int_0^m r^2 dm \tag{4}$$

where m is the mass at any location and r is the distance between the axis under consideration and the mass. Therefore, the farther away the mass is from the axis of rotation, the harder it is to change the rate of rotation of the object. The integral form of the MOI in Eqn. 4 is used for a continuous mass, where the infinite sum of all point mass moments will give the MOI of the whole system.

Two bats of equal mass and length may have different MOI values depending on how the mass is distributed along the length of the bat. The MOI value also varies depending on the axis under consideration. Nathan [10] has considered two cases in which he changed the MOI of the bat by decreasing the thickness 10% thinner and adding additional 2.3-oz weight either at the barrel (barrel or tip loaded) or at the knob (knob loaded). All the other parameters in the calculations were kept the same. These bats were

modeled so that the total weight of the bat remained the same and only the mass distribution varied. From his models, he concluded that the barrel-loaded bat outperforms the knob-loaded bat when they are swung at the same speed. The reason for the higher performance of barrel-loaded bat can be explained by the fact that in the case of the barrel-loaded bat, there is more mass in the vicinity of the impact location than in the knob-loaded bat. With the swing speed being kept constant, the increase in mass in the barrel and consequently increasing the MOI increases the initial momentum, and hence, the final ball exit velocity. However, with change in MOI, the swing speed of a bat varies. Nathan [11] developed an equation to calculate the change in swing speed of a bat as a function of change in MOI, which is given as,

$$\Delta swingspeed = 1.2X10^{-3}(mph/(oz-in^2))X\Delta MOI@knob \quad (5)$$

which enables the calculation of change in swing speed with corresponding change in MOI.

3.2.4 Center of Percussion

The motion of the bat after collision involves rotation, translation and vibration. The center of percussion (COP) is the impact point on the bat that produces minimal reaction to the batter's hands. The concept of COP can be understood from a discussion presented by Cross [12] in regards to a tennis racquet. Consider a baseball bat supported at the knob by a string. When the ball impacts the bat at any point other than its center of gravity, there is a reaction impulse along the length of the bat in the form of bat recoil and rotation. The recoil causes the bat to move away from the ball, whereas the handle of the bat tries to move closer to the ball. If at any point, these two opposite effects are equal

to each other, then that point will remain stationary and the bat will rotate about this point. This impact point is called the Center of Percussion, and the point where the two forces cancel each other is called the conjugate of the COP. When a bat is normally gripped, the COP is between 6 to 8 inches from the tip of the barrel. Therefore, when the impact occurs at the COP, the batter does not feel any sting on his hands, as they coincide with the conjugate of the COP.

From a study by Noble [13], COP can be calculated as

$$COP = \frac{MOI}{m * r} \tag{6}$$

with the mass moment of inertia (*MOI*) of the bat about the center of mass (CG), the mass of the bat (*m*), and the distance (*r*) from the axis of rotation to the CG.

The center of percussion is often misunderstood by the player as the sweet spot (location on the bat producing maximum-batted ball velocity). However, the sweet spots and COPs on bats are very close to each other but are not necessarily at the same position on the bat. A study by Weyrich [14] demonstrated that the COP is the impact location that produces the greatest ball-exit velocity with a stationary bat. However, these results cannot be taken as a standard because a stationary bat cannot completely explain the dynamics of a bat that is swung. Also a theory developed by Brody [15] to determine the impact location on the bat that would result in the greatest post-impact velocity shows that this location is not on the COP but is a function of velocities of the bat and ball, their mass and also the inertial and material properties of the ball.

3.3 MODAL ANALYSIS

Knowledge of the dynamic properties of any structure is important to understand its behavior when subjected to dynamic loads. The dynamic characteristics involve natural frequencies, damping and mode shapes of the structure. Structures undergo elastic deformation or vibrate when a dynamic load is applied. The COP of a baseball bat is explained based on the assumption that the bat is completely rigid. However, in reality, a baseball bat is similar to a free-free beam, and the brief duration of contact with the ball is short enough to excite the vibrations in the bat.

Modal analysis is a procedure, which describes a structure in terms of its dynamic characteristics. The procedure involves exciting the vibrations in the structure under consideration by applying a dynamic load to it. The structure is excited by hitting it with an impact hammer or by using a shaker. The response of the structure is recorded as a time trace using an accelerometer. The time trace shows the response of the structure to the applied force in the time domain. In Modal Analysis, this time-domain response is then transformed into the frequency domain by using Fast Fourier Transformation (FFT), and the Frequency Response Functions (FRFs) are computed. The FRFs show the response of the structure in terms of the frequency domain. The FRFs also have peaks in the frequency plot which correspond to the peaks in the time trace. These peaks correspond to the natural frequencies of the structure. Therefore, the FRFs can be used to obtain the natural frequencies of the structure directly.

The mode shapes can also be obtained by collecting many FRFs on the structure along its length. The amplitude of the FRF at the resonant frequency is directly related to the mode shape.

3.3.1 Vibrations in the Bat

When it comes to the vibrations of the bat, three important questions have to be answered. One fundamental question is: Are the vibrations in the bat good or bad? Because vibrations are a measure of stiffness, what effect does the gripping of the batter's hands around the handle have on the vibrations of the bat? What is a node point? and how is it related to the sweet spot or the overall performance of the bat? These questions can be answered by understanding the dynamics that occur during and after the collision.

The vibrations of a bat can be compared to that of a free-free beam. Research by Brody [16] has shown that the hand-held grip does not significantly change the frequencies and mode shapes of a bat but only dampens the vibrations quickly. Therefore, a free-free bat is sufficient to explain the vibrational behavior of a hand-held bat.

The frequencies of vibrations influence the performance depending on the period of oscillation and the contact time between bat and ball. The impact of the ball distorts the bat. Some energy is lost in this distortion. Depending on whether or not the half-cycle period of oscillation of the bat is longer than the contact time, the distortion energy is either retained in the bat as vibrations or returned to the ball [3]. In quantitative terms, the fundamental frequency of the 33-in. metal bat used in this research is 200 Hz, and the contact time is ~0.001 s. Because the half cycle of the period of oscillation in this case, which is ~0.0025 seconds is relatively longer than the contact time, the bat may not return the energy of distortion to the ball but may retain it as vibrational energy. Therefore, in this case the vibrations in the bat decrease the ball exit velocity—provided the impact is not at a node point.

A node point is the location where the amplitude of vibration is zero. Therefore, an impact at a node point will cause minimum vibration in the bat. Hence, less energy is lost in the bat vibration, and more energy will be transmitted to the ball. The node point of the fundamental vibrational mode is normally found between 5 to 7 inches from the tip of the barrel of the bat. Cross [12] has defined the region between the two fundamental nodes of a bat (Node 1 and Node 2 described in Chapter 2) as the 'sweet zone' for impact which will cause minimum vibrations in the bat and maximum energy is transferred to the ball—giving an optimum exit velocity. It was also observed from a study by Van Zandt [17] that the ball exit velocity is relatively lower at any location other than the node point. Apart from the nodes and bending vibrations, the trampoline effect or breathing mode of the barrel of a metal bat has a significant influence on the performance [18]. Russell [18] has done research on the vibrational properties of the bat and has concluded that the performance of an aluminum bat decreases with increasing hoop frequency, which is attributed to the trampoline effect.

3.4 Finite Element Analysis

The knowledge of deformations, stress-strain patterns, temperature flow or fluid flow in any system subjected to an external loading or pressure is essential for its best design. Engineers are interested to know what will be the effect of the applied load on any system. Often, it is hard to evaluate the system as a whole. The Finite Element Method (FEM) or Finite Element Analysis (FEA) enables dividing the system into small sections and analyzing each section. These tiny sections or elements make up the system as a whole. The corners of the elements are called nodes. The degrees of freedom, which are the number of independent movements possible, are represented by the nodes. The

type of elements to be used depends on the characteristics of the original structure. For example, for a one-dimensional structure, line elements will be used and for two-dimensional structures, triangular or quadrilateral elements will be used. Once the relevant types of elements are defined, the corresponding material and geometrical properties associated with the elements are defined. Proper boundary conditions, which completely describe the constraints for the problem at hand, are then applied to the system. Relevant equations are generated by specifying the corresponding loads. These equations are then solved first for primary unknowns (displacements and reaction forces) and then for secondary unknowns (stresses and strains). These results are generated for each node, which is an advantage with discretization. Finite Element software like HyperMesh® and LS-DYNA© reduce the cumbersome hand calculation of all the equations and provide a computed result. With the new technology, the scope of interpretation of results has also increased significantly over what was available even 10 years ago because of various graphing tools available.

FEA involves three stages: (1) Preprocessing, in which the basic geometry is created and the relevant loads, boundary conditions and material properties are defined. A preprocessor generates an FE file for further processing, (2) Analysis, in which the associated equations are solved and results are generated. The output file from the pre-processor is input to the finite element solver. The solver also generates a series of output files for interpretation of results, (3) Postprocessing is the stage where the results are transferred into a form that is easy to interpret. All the solver generated files will be analyzed and necessary graphs and tables will be created.

The disadvantages associated with FEA are that the responses of the structure or the results are highly dependent on the boundary conditions and loads specified and, depending on the complexity of the problem; the calculation can consume significant computer resources.

3.5 PREVIOUS RESEARCH

Brief descriptions of the research done by other baseball-science experts that are used in this thesis will now be discussed.

Van Zandt [17] did significant research on baseball. In his paper [17], he modified the standard theory of beams to consider the nonuniform structure of a baseball bat. He calculated the normal modes for bending vibrations of the bat and solved the collision problem by including the effect of vibrations of the bat on the flight of the ball. One interesting result from Van Zandt's work is the calculation of ball exit speed as a function of impact position along the length of the bat. His studies also showed that impacts at any point other than the node will yield a relatively low performance.

Nathan documented his work on baseball in two publications. In his first publication [19], he developed a collision model between ball and bat. His model shows that vibrations play an important role in determining the ball exit speed. One very important conclusion from his model was that any effect of clamping action of hands at the end of the bat is felt at the impact point only after the ball leaves the bat. Therefore, for all testing and modeling purposes, a free-free boundary condition of the bat is a legitimate approach.

In another paper by Nathan [10], he defined a set of laboratory measurements that can be used to predict the performance in the field. Using a computational model, he showed that the bat performance depends on the elasticity of the ball-bat collision, the inertial properties of the ball and bat and the bat swing speed. One interesting result from his comparison between knob-loaded and barrel-loaded aluminum bats is that the barrel-loaded bat performs higher than a knob-loaded bat. This higher performance is because of the presence of more mass in the vicinity of the impact in case of a barrel-loaded bat.

Noble [13], summarized the work of many researchers on the various factors relevant to the design and performance of baseball bats. He identified mass, MOI, coefficient of restitution, location of the node of the fundamental vibration mode and the COP location as the inertial and vibrational factors relevant to the bat design and performance. Some interesting results from his work are:

- COP impacts are more comfortable than impacts at other locations because there is no painful impact/shock as is experienced during impacts at other locations. He also mentioned in this paper that the COP has been demonstrated to be the impact location producing the greatest post-impact velocity with a stationary bat.
- During impact, the vibrational behavior of a bat is more like a free unsupported bat, regardless of the firmness of the grip. Therefore, a free-free model of testing the bat for its frequency response is again stated to be legitimate.

Two important conclusions from his work, regarding the vibrational properties of the bat are:

- Post-impact velocity is significantly lower for impacts not on the node, especially as the impact location moves toward the handle of the bat.
- When using bats with the node and COP close together, impacts at both locations are more comfortable than at other locations, with no significant difference between the two. However, if the COP was moved away from the node, impacts at the node were more comfortable than impacts at any other locations including the COP.

Smith, Shenoy and Axell [20] developed a finite element model to predict the performance of wood, metal and composite baseball bats. This model was used to study the influence of impact location, bat composition and impact velocities. They used a viscoelastic ball model, which captures the time-dependent properties of baseballs. The study demonstrated that the performance of a metal bat (aluminum) depends on wall thickness.

Mustone and Sherwood [21] developed a finite element model to predict the performance of baseball bats. Mass, MOI, CG were calculated experimentally. The sweet spot on the bats was obtained using a hitting machine. Frequencies of the bats were obtained by conducting modal tests on the bats. HyperMesh® was used for building the geometries of the wood and aluminum bats, LS-DYNA© was used for analysis, and LS-Post and the ETA Postprocessor were used for postprocessing. The finite element models of the baseballs were calibrated by impacting the ball against a stationery wooden block at 60 mph and adjusting the material properties of the ball so that the COR of the

ball was 0.55. The bat models were calibrated by comparing the mass, MOI, center of gravity and the vibrational properties (natural frequencies) of the bats with experimental values. Differences between wood and aluminum bats in terms of performance and contact time were studied. Two important conclusions from their study were:

- There was no difference in the batted-ball velocity when the bat was given a purely rotation or purely translational motion towards the ball.
- Modal Analysis was an effective tool for the calibration of FEA models to predict their batted-ball performance.

3.6 SUMMARY

With this background, this research is aimed at studying the design parameters of bats and their effects on performance. Two bats, one aluminum and one wood, were selected for the research and were subjected to experimental calculations and finite element analysis to compare their performance. Then, a parametric study was done on the aluminum bat to study the design parameters.

4 EXPERIMENTAL METHODOLOGY

This research involves experimental and finite element studies of the design parameters of aluminum bats. The procedures or methodology followed for the experimental measurements are described in this section. A 33-in. aluminum and wood bat were selected for the research. Prior to the performance testing of the bats, the mass, MOI and CG on the bats were measured according to NCAA standards. The barrel diameters and the wall thickness (aluminum bat) were also recorded. The procedures/standards for these measurements are illustrated in the following sections.

4.1 MASS AND CENTER OF GRAVITY OF THE BAT

The masses of the bats were measured to the nearest 0.005 oz using a digital scale. The bat lengths were also measured to the nearest 1/16 in. The CGs were measured by balancing the bat on a knife-edge as shown in Fig. 2.

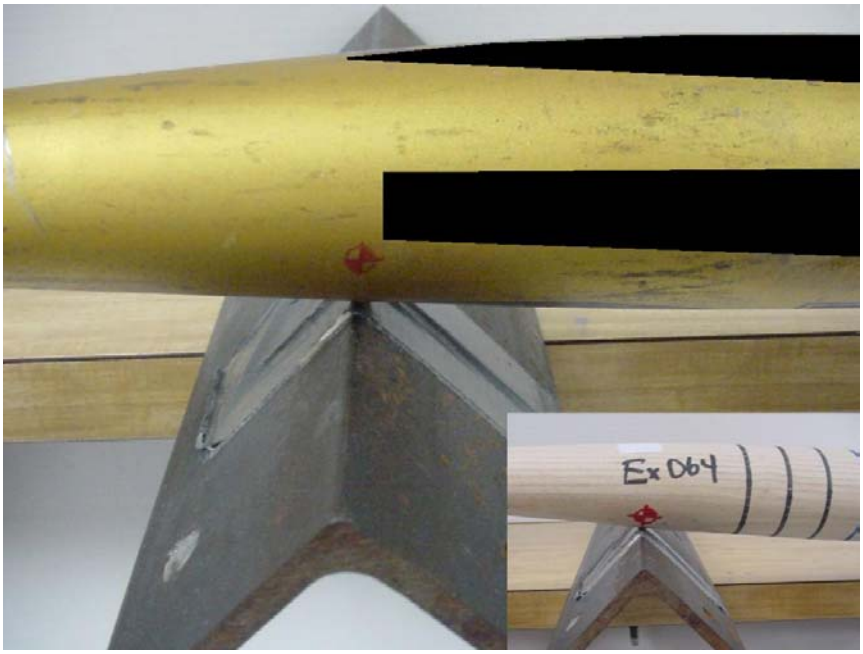

Fig. 2: Measurement of the CG of the bat

4.2 Moment of Inertia

The moment of inertia was measured according to the *ASTM Standard* [22]. To calculate the MOI, the average period of the bat to be used in the calculation of the MOI is first measured.

4.2.1 Average Period

To calculate the average period, the bat is clamped at the handle and is suspended to rotate freely about a pivot (as shown in Fig. 3). Fig. 3 shows the MOI setup for wood and aluminum bats. The inset in Fig. 3 shows a zoom in view of the bat pivot point. The bat is centered about this pivot point. The bat is given a small rotation (less than 15°) from vertical and is released to swing freely. Once the bat settles in oscillation, the time taken for 40 full cycles is measured using a stopwatch or with an oscilloscope. The test is repeated three times to minimize any errors. The average period of the bat is then calculated as,

$$averageperiod = \frac{\sum_{1}^{n} \frac{time}{no.of.cycles}}{no.of.tests} \tag{7}$$

Once the average period of the bat is calculated, the moment of inertia of the bat is calculated using the formula,

$$I_{pivot} = \left(\frac{\left(averageperiod^2\right) gWa}{4\pi^2} \right) \tag{8}$$

where:

I_{pivot} is the Moment of Inertia about 6 in. from the point of suspension (oz-in^2)

W is the bat mass (oz.)

a is the distance from pivot point to center of gravity (in.)

Fig. 3: Measurement of MOI of the bat

4.3 CENTER OF PERCUSSION

According to the *ASTM Standard [22]*, the COP of the bat can be calculated as

$$COP_{axis} = \left(\frac{averageperiod^2 g}{4\pi^2} \right) = \frac{I_{axis}}{W * a} \tag{9}$$

The COP about any point on the bat can be calculated using Eq. (9). However, the value of the moment of inertia, I_{axis}, will change depending on the point selected for the axis of rotation.

Once the COP about a point is calculated using Eq. (9), its distance from the tip of the barrel can be calculated by subtracting it from the length of the bat. For example, the COP about the axis can be first calculated using Eq. (9) and its distance from the tip of the barrel can then be calculated as,

$$\text{COP}_{\text{(from barrel end)}} = L - d_{axis} - COP_{axis} \tag{10}$$

where:

L is the length of the bat (in.)

d_{axis} is the distance of the axis from the knob end of the bat (in.)

4.4 Barrel Diameter and Wall Thickness

The diameter of the bat is measured using vernier calipers at every inch starting from the tip of the barrel to create the bat profile for use in creating the FEA models. The diameter at one location is measured and then the bat is rotated 90° and another measurement is taken again at that same axial position on the bat. The average of these two values is used as the diameter at that axial position of the bat for creating the profile.

The wall thickness of the aluminum bat is measured at every inch starting from the barrel end of the bat using an ultrasonic thickness tester (Fig. 4). Prior to the measurement, the initial velocity of the apparatus is set to the velocity of sound through the medium being measured. In the case of an aluminum bat, the medium is Aluminum C405, and the value of velocity (V) is 0.25257 in/μs. The thickness tester has a sensor which when placed on the medium being measured, sends a sound impulse through the material. The impulse is reflected when there is a change in the medium, i.e. from aluminum to air. The time taken for the impulse to travel in (T_1) and out (T_2) are recorded. The thickness of the bat is then calculated using the formula,

$$\text{Thickness, } t = \frac{V*(T_2 - T_1)}{2} = \frac{0.25257*\Delta T}{2} \tag{11}$$

The wall thickness of a 33-in. aluminum bat used in this thesis varies from 0.12 in. at the barrel and decreases to 0.092 in. at the throat and increasing to 0.11 in. at the handle.

Fig. 4: Measuring the wall-thickness of aluminum bat

4.5 BALL COR MEASUREMENT

The coefficient of restitution (COR) of the ball is defined as the ratio of the output velocity of ball to the inbound velocity. The COR is a measurement of the liveliness or bounciness of the ball. For the same test conditions, a ball with a high COR produces a higher ball exit velocity than a ball with lower COR.

Prior to testing for COR, the mass and the moisture contents of the balls are recorded. The balls are impacted against a stationary steel block, 2-in. thick, 12-in. wide and 12-in. high. The balls are pitched at a speed of 60 mph by a pitching machine (Fig. 5). The velocity of the ball before the impact (V_1) and the velocity of the ball after impact (V_2) are recorded. The COR of the ball is then calculated using the formula,

$$\text{Ball COR} = \frac{-V_2}{V_1} \tag{12}$$

Different pitching speeds, ranging from 30 to 100 mph, were also used in this thesis to get the COR of the ball at different speeds. A curve of COR vs. pitch speed was then drawn to understand the performance of ball. These data are later used in the calibration of finite element model of baseball.

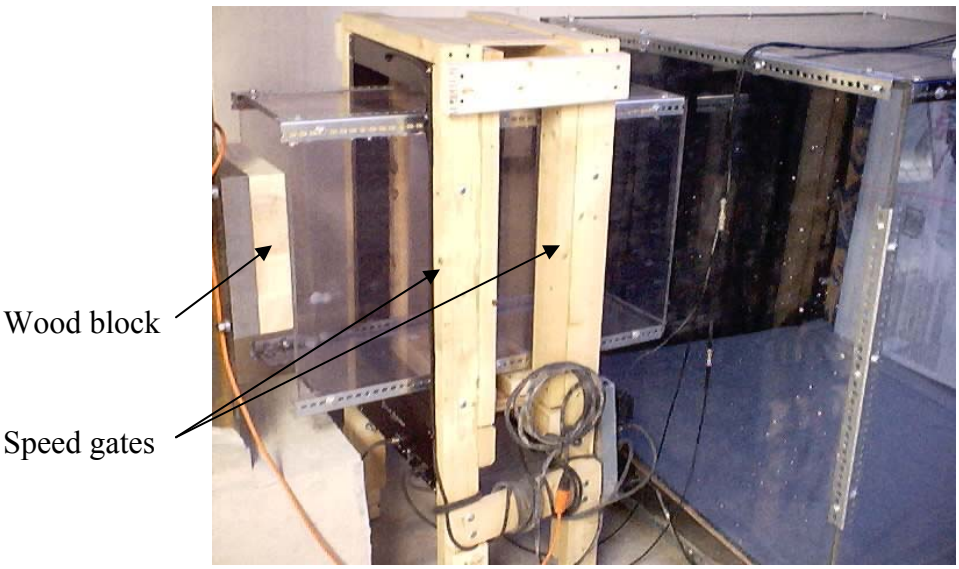

Fig. 5: COR testing of baseball

4.6 BAT TESTING

Once the mass, CG and MOI measurements are recorded, the bat and the ball are mounted in the BHM [23] (shown in Fig. 6). The ball is given an initial velocity of 70±2 mph and the bat is swung at a velocity of 66±1 mph (at the 6-in. location from the tip of the barrel).

The bat swing speed depends on the point of contact/impact location. The swing speed at the point of contact is calculated using [23],

$$V_{contact} = 66.\left(\frac{(Batlength - 5.375 - Location)}{(Batlength - 11.375)}\right) \quad (13)$$

where $V_{contact}$ is the velocity at the contact point (mph)

Batlength is the overall length of the bat (in.)

Location is the distance of the impact point from the tip of the barrel (in.)

The torque supplied to the bat is cutoff at about 12.8 inches prior to the point of contact to accommodate coasting during contact and to avoid the servomotor powering the bat through the collision. The ball must pass through an exit hole and the target, which is a diamond with 13-in. long diagonals (shown in Fig. 7), is 62-1/16 in. from the impact point. All measurements are taken from the barrel end of the bat. The ball exit velocities are measured at a distance 9-10 in. and 13-14 in. from impact during the test. The test is started by impacting the bat at the 6-in. location. After the velocities are recorded, the test is continued at the 5-in. and then at the 7-in. locations. If necessary, the test is conducted at additional locations with 1-in. or 0.5-in. increments, i.e. five consecutive (five for aluminum bats only, in the case of wood bats, only three consecutive valid readings are recorded) *valid hits* are recorded at each of the impact locations. According to the NCAA protocol [23], "A hit is declared valid if the ball exit speed at the 72-inch gate location is less than the higher of the speeds as measured at the 9- and 13-inch light cell positions". The testing is continued until the average of the five consecutive readings at any impact location is greater when compared to the

½-in.locations on either side. For example, the test is halted if the average velocity at the 5.5-in. location is greater than the average values at the 5.0- and 6.0-in. locations. The location at which the impact gives the highest ball exit velocity (average of 5 valid hits) is recorded as the 'sweet spot'.

Fig. 6: Bat and ball mounted in the Baum Hitting Machine

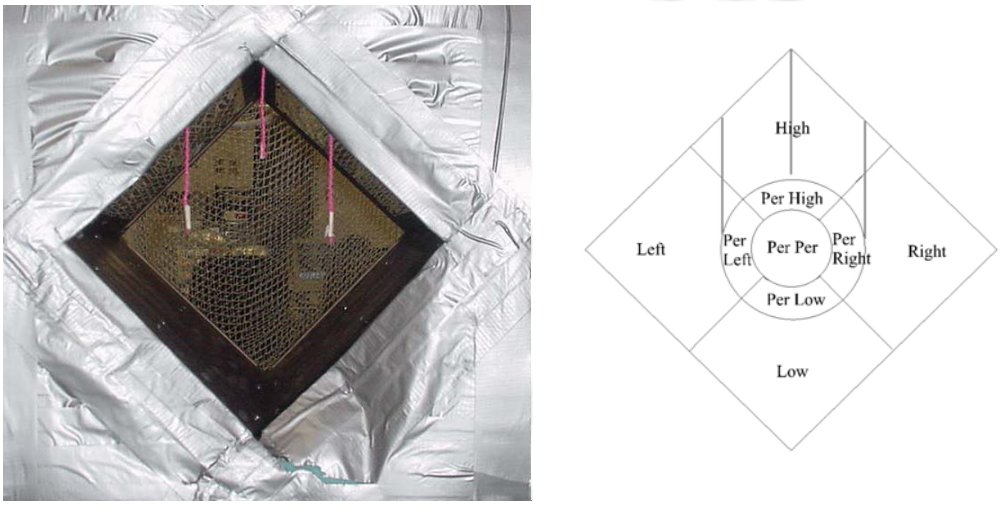

Fig. 7: Baum Hitting Machine – target View

Fig. 7 shows the target view of the BHM. The figure to the right shows the notations for the different areas of the target that are recorded depending on the exit positions of the ball.

4.7 Frequencies and Node Points

Modal testing is done on the bats to calculate the frequencies, node points and mode shapes. The bat is hung with strings near the ends so that an essentially free-free boundary condition can be maintained. The accelerometer is placed near the barrel end of the bat. The bat is hit at several locations using an impact hammer (Force location is varied and the response location is kept constant) and the reaction at each of these locations is measured using the accelerometer (parallel to the direction of force). The setup for modal testing is shown in Figs. 8 through 10. The analyzer used and the test setup are listed in Table 1.

Fig. 8: Modal testing setup

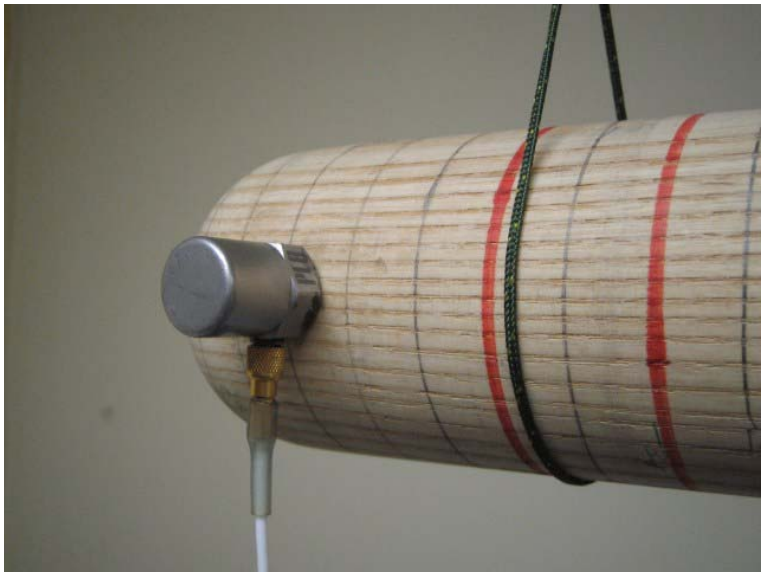

Fig. 9: Accelerometer location on the bat

Fig. 10: FFT analyzer

Table 1: List of apparatuses used for modal testing

Analyzer Model	HP35665A
Accelerometer Serial No	PCB 303A02 S/N: 17771
Hammer Serial No	PCB 086 B03 S/N: 2057
Channel	Hammer
Channel2	Accelerometer
Number of Averages	3

The frequencies are measured up to a span of 800 Hz with 400 spectral lines. The frequencies are identified by observing the imaginary part of the FRFs. The cursor on the screen is moved to the peak (highest point) of the first curve in the FRF, and the frequency at that value is recorded as the frequency at which the first bending mode appears.

The mode shapes are identified by impacting the bat at every inch (33-points) along its length and plotting the maximum amplitudes at each location. For example, to plot the first mode shape, the bat is impacted at every inch starting from the barrel end. After impacting each location, the amplitude of the peak (highest point) of the first curve

in FRF is recorded. The 33 amplitude values on this 33-in. long bat are then plotted as a function of location to get the first mode shape.

The node points on the bat are identified by finding the point of zero amplitude. For example, the barrel of the bat is impacted and the point on the barrel, which gives zero amplitude for the first mode, i.e. the curve for the first bending mode, does not appear in the FRF, is recorded as the barrel node point for the first bending mode.

The bats are then rotated by 90 ^{o} and frequencies are again measured to check for symmetry. In the case of wood bats, measurements are taken along the grains and perpendicular to the grains. Figs. 11 and 12 show the two positions of the wood bat.

Fig. 11: Along the grains

Fig. 12: Perpendicular to the grains

4.8 Performance Curves

Once all the experimental calculations are done, the performance curves for the wood and aluminum bats are drawn. The performance curves are plotted with the ball exit velocity on the y-axis and the location of impact on the x-axis. The performance curves show how the ball exit velocity varies with the location of impact on the bat.

4.9 Summary

Experimental calculations are performed on wood and aluminum bats. From the BHM testing it was observed that ball exit velocities off the aluminum bat are higher than wood bat. Modal test results also show higher frequencies for aluminum bat. Finite element models of the bats are then made and calibrated to the experimental values.

5 FINITE ELEMENT MODELING

Finite element models of the bat and ball were built to perform a parametric study of the bat properties. A brief description of the fundamentals of Finite Element Analysis (FEA) is mentioned in Chapter 2. The different models of bats (wood and aluminum) and balls used in this research are explained in this chapter. Necessary changes or improvements performed to the models during the course of thesis are also included in this section.

5.1 METHODOLOGY

In this chapter and throughout this research, the performance of the bat means ball exit velocity. Finite element models of 33-in. aluminum and wood bats are built and calibrated by comparing them to the experimental values.

HyperMesh® was used for preprocessing, i.e. building the geometry and the finite element model with the LS-DYNA© keyword template and as a postprocessor. Geometry and boundary conditions are defined in HyperMesh® using collectors. A material collector is used to define the type of material to be used, i.e. elastic, plastic, etc. and the material properties like density and Young's modulus are also defined in this collector. A properties collector is used to define the type of elements to be created and to select the material associated with these elements. Components (Comps) collectors are used to group all the properties, i.e. type of elements, material used and also to define other parameters like damping associated with these elements. The geometry and the elements

are identified by components collectors. This grouping of all elements into one collector enables defining a global constraint or applying a load on all the elements in that collector. LS-DYNA© by Livermore Software Technology Corporation was used for the finite element solver. LS-DYNA© has a large selection of material types, which can be used to capture the time-dependent material behavior of the ball in the finite element model. LS-Post and ETA postprocessors were used for post-processing.

5.2 Aluminum Bat Model

A finite element model of the aluminum bat was built after a production model 33-in, aluminum bat. Elastic properties of C405 alloy aluminum were used for the bat material. Material type 1 (listed in Table 2) in HyperMesh®, which is isotropic-elastic, was used for the bat material. Material type 3 which is isotropic-elastic-plastic was used for modeling the end cap (listed in Table 3). The properties of the end cap were supplied by the bat manufacturer. Thin shell elements were used for building the model. The diameter of the bat at every inch was measured and was used for creating the outer profile of the bat. The outer diameter profile was rotated 360° to get the surface of the bat. This surface was meshed using elements with an aspect ratio of ~2:1 to create the geometry of the bat. The bat was built with a uniform thickness of 0.11 in. and with two components: the bat and the end cap (Model 1). Figs. 13 thru 16 show the process of building the FEA model of the aluminum bat.

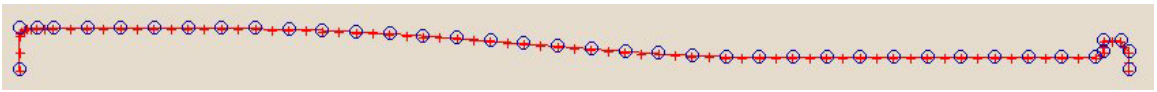

Fig. 13: Outer diameter profile of the aluminum bat

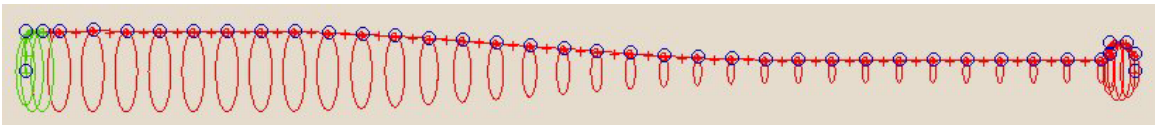

Fig. 14: Rotating the lines to create the surface of the bat

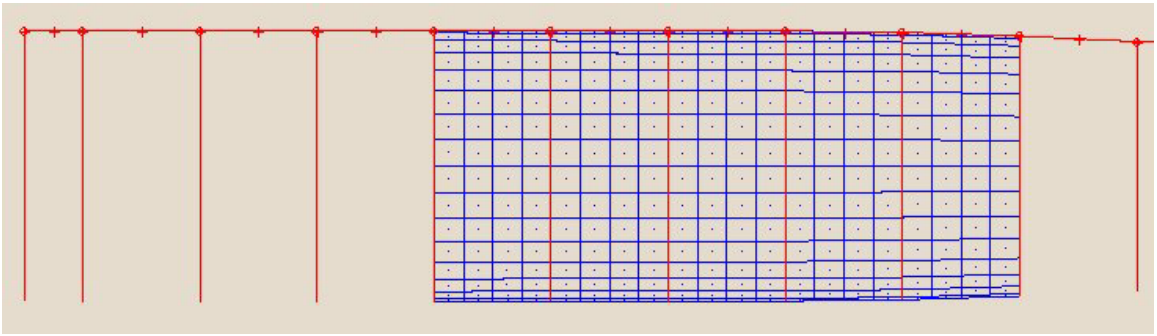

Fig. 15: Meshing the surface of the bat

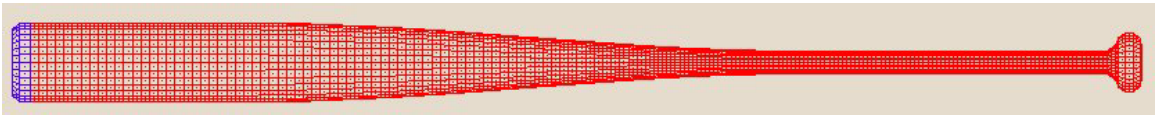

Fig. 16: Completed FEA model of aluminum bat

Table 2: Aluminum bat material properties

Aluminum bat		
Young's Modulus (psi)	Density (lb/in^3)	Poisson's ratio
$10x10^6$	0.1	0.33

Table 3: End cap material properties

End cap			
Young's Modulus (psi)	Density (lb/in^3)	Yield stress (psi)	Poisson's ratio
37,000	0.096	12,950	0.00

5.2.1 Calibration of Aluminum Bat

Once the bat model was built, the mass, moment of inertia, center of gravity and center of percussion of the model were recorded and compared with experimental values for calibration. The eigen-analysis of the bat is also done to calibrate the dynamics of the model to that of the actual bat. Eigen-analysis was done using the eigen-option in LS-DYNA© and the natural frequencies, mode shapes and node points were extracted.

The results from the FEA model with only two components (Model 1) did not match well with the experimental values. There was deviation in the MOI, CG and COP values. The frequencies and node points obtained also differ from the experimental values. Slight differences in the geometry and mass distribution can cause differences in frequencies. Another reason for the difference in the frequencies might be the variation in the wall thickness. The wall thickness of the actual bat varies along the length of the bat, and the first model was made with uniform thickness. Due to the differences between the experimental and FEA values, the model was further tuned in an effort to match better with the experimental values. A new bat model (Model 2) with five different sections (cap, barrel, throat, handle and knob) was built. The wall thickness for each of the sections was input by averaging the measured thickness values along those sections. The revised bat model is shown in Fig. 17. The eigen-analysis of this revised model was done

and the resulting frequencies and mode shapes were compared with the experimental values for calibration.

Fig. 17: Modified aluminum bat model (Model 2 - Five components)

The results from the revised model gave better correlation to the experimental values than Model 1 (Uniform Thickness). There were still differences between the experimental and FEA models, which indicated the need for further tuning of the model. A new model of the bat was built using 34 components, 33 for the bat and one for the end cap (Model 3). The experimentally recorded wall thickness at every inch on the bat model was used for the thickness for each of these components. This model correlated well with the experimental values and was therefore used for the parametric study.

5.3 WOOD BAT MODEL

The wood bat model was built in HyperMesh® using solid elements. The orthotropic elastic material in LS-DYNA© (HyperMesh Material Type 20) was used for building the wood bat. The outer diameter of the wood bat was measured at every inch on the bat. A profile of the bat was created using these measurements and a shell mesh was created. These shell elements were rotated 360° to get a solid mesh. However, a 360° rotation of the rectangular or 4 node elements resulted in wedge elements at the edges and a complete solid mesh of hex elements was not possible. Therefore, the outer profile for the wood bat was created by leaving a gap of 0.1 in. between the outer profile

and the centerline. The shell mesh was then created with these lines, and it was rotated 360°. The result was a solid mesh of the bat with a hole in the middle running uniformly along the whole length of the bat. The surface of this hole was meshed, and it was extruded along the length of the bat to obtain the complete solid mesh of wood bat with only hex elements. The shell mesh was deleted after the solid mesh was created and any cracks in the model were eliminated by deleting the edges. The properties used for the wood bat are shown in Table 4. The completed wood bat model is shown in Fig. 18.

Table 4: Wood bat material properties

Wood bat [17]									
Young's Modulus (psi)			Density (lb/in^3)	Poisson's Ratio			Shear Modulus (psi)		
E1	E2	E3	Rho	Pr1	Pr2	Pr3	G1	G2	G3
25E5	9E5	1.7E5	0.026	0.027	0.044	0.067	1E5	3.4E5	1.3E5

Fig. 18: FEA Model of Wood Bat

5.3.1 Calibration of Wood BAT

The wood bat model was calibrated by performing an eigen-analysis of the bat. Results from the eigen-analysis, i.e. the frequencies and mode shapes, were compared with experimental values. Properties of wood material were tuned to calibrate the model. Once the bat models were calibrated, the ball model was built and calibrated for contact analysis between bat and ball.

5.4 BALL MODEL

A baseball is made up of three different layers of yarn and has cork in the middle. It is covered with stitched leather on the outside. Fig. 19 shows the cross-section of a baseball.

Fig. 19: Cross-section of Baseball

A baseball is a viscoelastic structure. There is a time-dependent energy loss associated with deforming the ball. A simple elastic material will not be sufficient to describe the dynamics of the mechanical behavior of the baseball during and after contact. The material properties are listed in Table 5.

Table 5: Baseball material properties

Ball [16]				
Mass Density (lb/in^3)	Short-time shear modulus (psi)	Long-time shear modulus (psi)	Decay constant	Bulk Modulus (psi)
0.0276	4498	1492	5025	13495

The geometry of a baseball is similar to a solid sphere and, therefore, has to be meshed with solid elements. A simple 360° rotation of 4 node elements is not possible as it would create wedge elements (as was discussed in the meshing of the wood bat).

Therefore, the geometry was created with a 0.2-in. diameter hole in the middle of baseball. Solid map, which allows surface to surface meshing, was then used to mesh one eighth of the volume of the baseball. This mesh was then rotated to obtain full mesh of a solid baseball. The process of creating the baseball geometry is shown in Figs. 20 through 22.

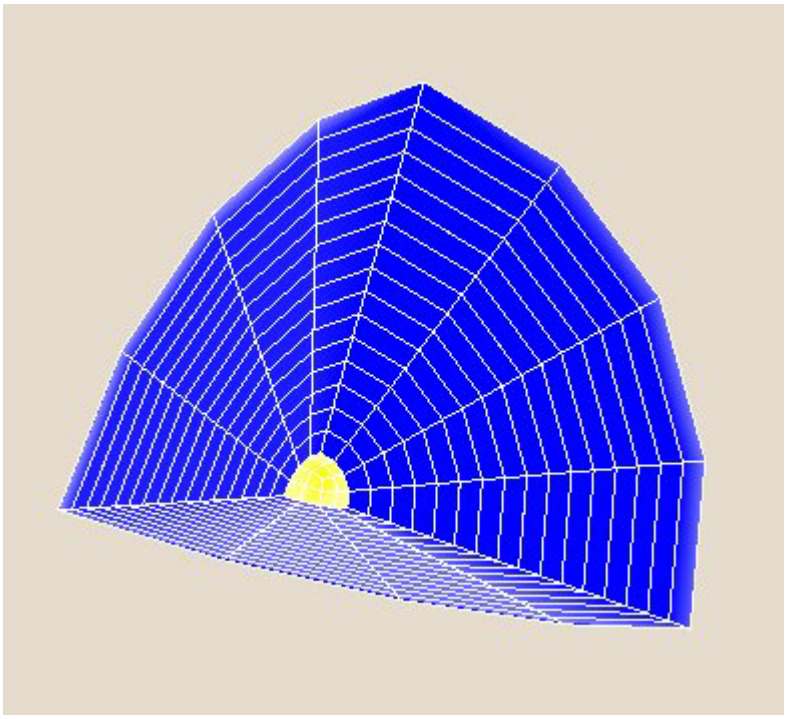

Fig. 20: Creating 1/8 of the volume of the ball

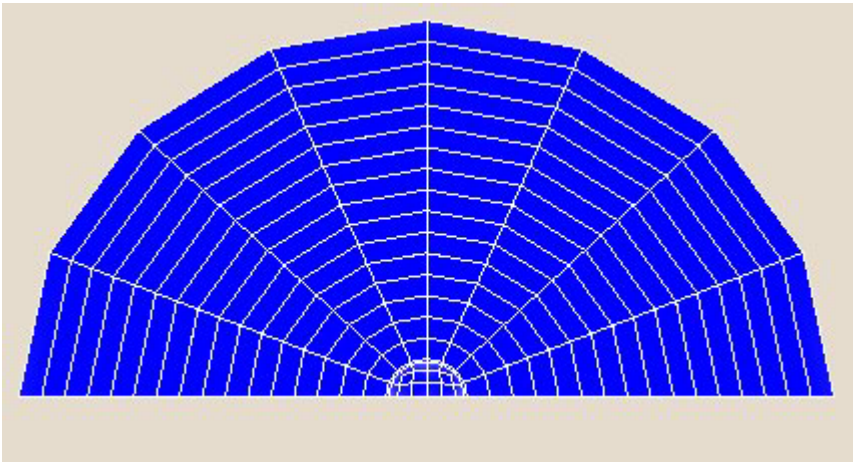

Fig. 21: Spinning the 1/8 volume to create ball geometry

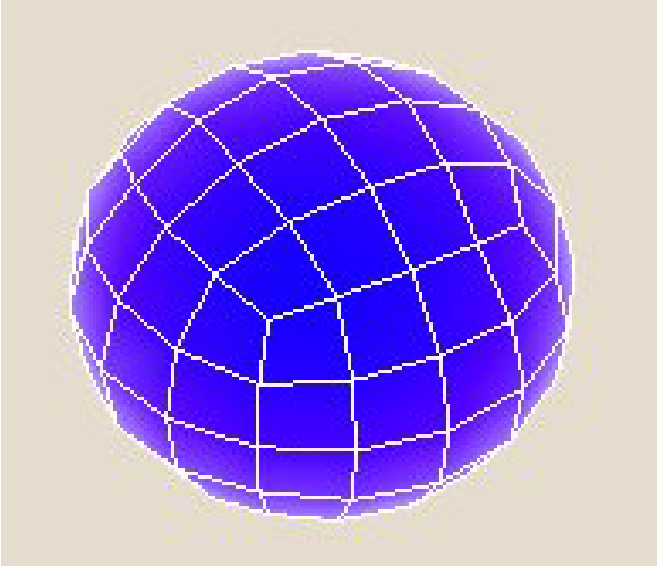

Fig. 22: Completed geometry of the ball

5.4.1 Calibration of Ball Model

Once the ball model was built, it was impacted against a fixed steel block at different speeds ranging from 30 mph to 100 mph and the COR of the ball was adjusted such that it fell in the experimental COR range of the two balls that were tested for all pitch speeds varying from 30 mph to 100 mph..

5.5 CONTACT MODELING

Contact between the ball and bat was defined using the Automatic-Surface-to-Surface contact algorithm in LS-DYNA©. The Surface-to-Surface contact algorithm requires a master surface and a contact surface. The master surface is the one, which is relatively more stable (i.e. fixed), than the slave. Therefore, in the contact between bat and ball, the bat was defined as the master and the ball as the slave.

5.6 Boundary Conditions and Loads

No constraints were defined either on the bat or on the ball. An initial velocity of 70 mph was given to the ball and a tip velocity of 85 mph was given to the bat. The velocity of the swung bat in the field is different at every location on the bat. The velocity at each point on the bat corresponding to a velocity of 66 mph at 6-inches from the tip of the barrel is calculated using a FORTRAN code. The FORTRAN program gives a velocity pattern which dictates a positive velocity for the bat barrel and negative velocity for the handle. This pattern is similar to the actual movement of the bat in the field. The ball is impacted on the bat first at 6 in. from the tip of the barrel, then at the 5.0-, 5.5-, 6.5- and 7.0-in. locations.

5.7 Postprocessing

Postprocessing was done using LSTC and ETA post-processing in LS-DYNA©. The ball exit velocity with respect to time was obtained from LSTC Postprocessing. Contact time, frequencies, mode shapes and displacements of elements were recorded using ETA Postprocessing.

5.8 Summary

Finite element models of wood and aluminum baseball bats and ball were built using HyperMesh® and LS-DYNA©. The models were compared and calibrated to experimental values using eigen-analysis. Surface-to-Surface Contact was defined between the bat and ball and ball exit velocities and contact times were recorded. Results of the FEA models will be discussed in the Results Chapter (Chapter 6).

6 RESULTS / DISCUSSION

The results of the experimental calculations and finite element modeling done in this research are presented in this chapter. Results of the parametric study of the finite element models of the bats are also presented in here.

6.1 EXPERIMENTAL RESULTS

Experimental results involve four sections; physical dimensions, ball exit velocities, modal test results and ball COR test results. These results for wood and aluminum bats are described in this section.

6.1.1 Physical Dimensions

Two bats, aluminum and wood, 33-in. long are selected for this research. The mass, MOI, CG and COP on these bats are presented in Table 6. The MOI listed in Table 6 is about the knob. The COP is measured from the barrel end and is about the axis i.e. 5.375 in. from knob end.

Table 6: Bat mass properties – experimental values

Bat Material	Mass (oz)	MOI@knob (oz-in^2)	CG (in)	COP (in)
Aluminum	30.695	16147	12.50	5.50
Wood	30.735	17369	10.88	6.35

6.1.2 Sweet Spot Locations

Ball Exit velocities of the two bats were determined experimentally by testing the bats in the Baum Hitting Machine. The exit velocities are listed in Table 7. Table 7 shows that the performance of the aluminum bat is higher than the performance of the wood bat. In addition, it is identified from Table 7 that the sweet spot (location of the maximum velocity) is at 6.0 in. on the aluminum bat and at 6.5 in. on the wood bat. Only three experimental measurements of the wood bat are listed in Table 7 as the sweet spot is at 6.5 in. location. BHM testing is normally started at 6.0 –in. from the tip of the barrel and is then impacted at 0.5-in. increments between 5 and 7 in. from the tip of the barrel until a maximum ball exit speed value is obtained. An impact location is identified as the sweet spot, or the location producing the maximum ball exit speed, if the ball exit speeds at 0.5-in. increments on either of this location are less than the ball exit speed value at this location. In this case, the test is started at the 6.0-in. location and then continued at the 6.5-in. location. Because a higher velocity is obtained at this location when compared to the previous location (6.0 in.), the test is continued on to 7.0-in. location. As the velocity at 7.0-in. location is less than the value at 6.5-in., the 6.5-in. location is recorded as the sweet spot and the test is halted.

Table 7: Ball exit velocities of wood and aluminum bats - experimental values

Location from barrel end (in)	Bat swing speed (mph)	Ball exit velocity [BEV] (mph)	
		Aluminum bat	Wood bat
5.0	66.00	91.656	-
5.5		93.576	-
6.0		95.231	92.195
6.5		94.761	92.587
7.0		91.944	91.112

6.2 MODAL TESTING

Modal testing is done on the bats to measure the frequencies, node points and mode shapes. The modal test results for both aluminum and wood bats are presented in this section. The test results are presented in the form of FRFs, mode shapes and tables.

6.2.1 Aluminum Bat

The FRFs of the aluminum bat are shown in Figs. 23 and 24. Fig. 23 was recorded by impacting the bat at a random location with a frequency span of 400 Hz (response is measured only from 0 to 400 Hz). The FRF was obtained with only one peak. This peak was observed at 198 Hz which corresponds to the fundamental frequency of the bat. The bat was then impacted throughout the length, and the amplitude of this peak at 198 Hz was recorded at each location to obtain the first bending mode shape. Fig. 24 is an FRF due to an impact at a random location on the bat, with a frequency span of 800 Hz. The two peaks that appear in Fig. 24 correspond to the first two frequencies. The second bending mode shape was obtained by impacting the bat throughout its length and by recording the amplitude of the second peak in the FRF at each location and plotting these values. Figs. 25 and 26 show the mode shapes for mode 1 and mode 2, respectively.

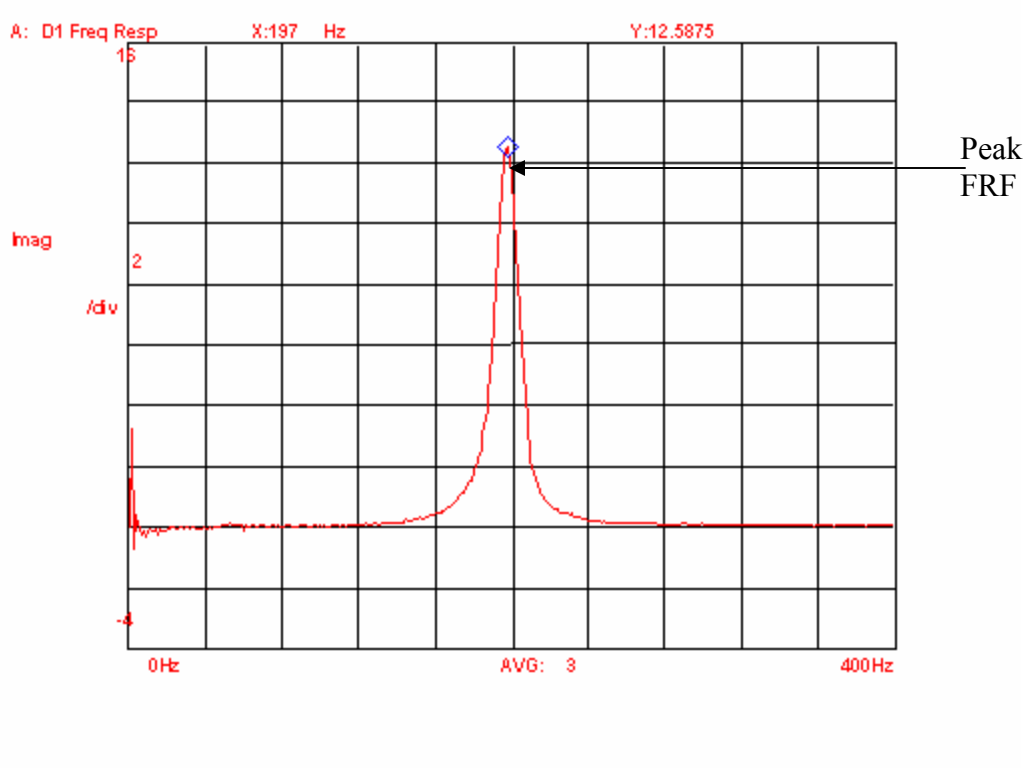

Fig. 23: Aluminum bat first bending mode

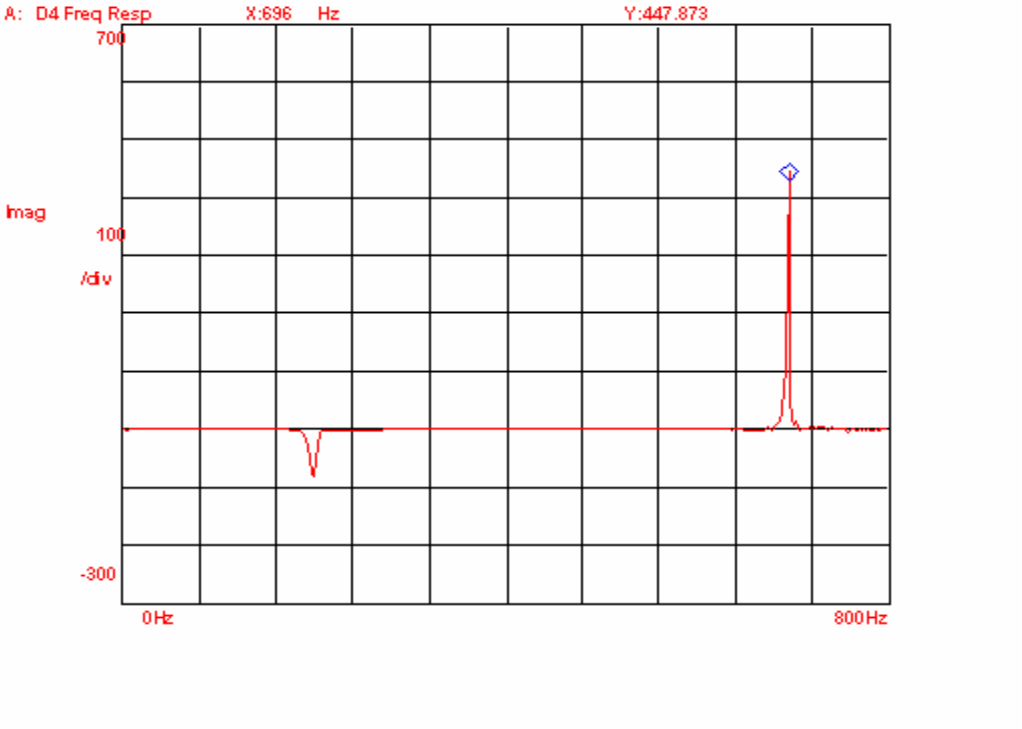

Fig. 24: Aluminum bat second bending mode

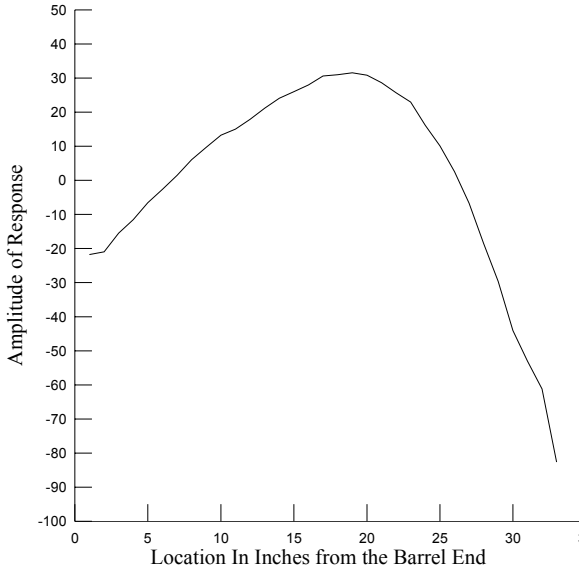

Fig. 25: Aluminum bat - first mode-shape plot-experimental

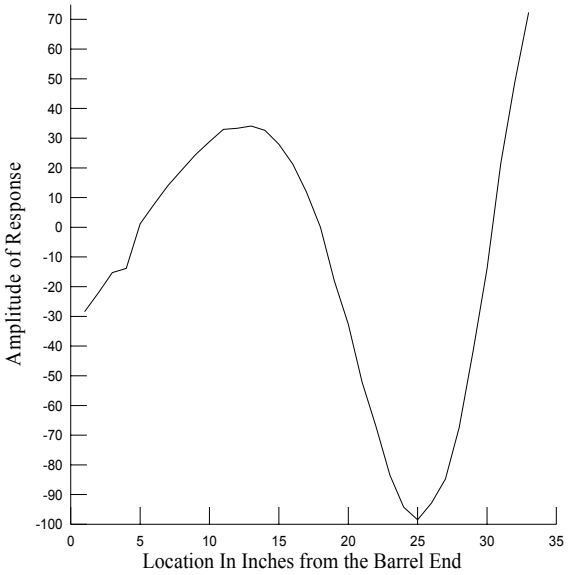

Fig. 26: Aluminum bat - second mode-shape plot-experimental

The nodes of the modes are the points of zero amplitude. These are identified on the bat by randomly impacting the bat and finding the locations where the peaks in FRFs have zero amplitude. For example, if impacting a bat at arbitrary locations gives FRFs with zero amplitude for the first peak (peak at 198 Hz), then these locations are identified as nodes of the first mode. Similarly, the impact locations that have zero amplitude for the second peak are identified as nodes of the second mode. The first mode of the bat has two nodes and the number of nodes increases by one for the next modes, i.e. the second mode has three modes and so on. However, only nodes close to the sweet spot are recorded in this research for the comparison purposes. Fig. 27 shows the FRF that corresponds to the node (only close to the sweet spot) of the first mode of the aluminum bat. Experimentally recorded values of frequencies and node points of the aluminum bat are presented in Table 8.

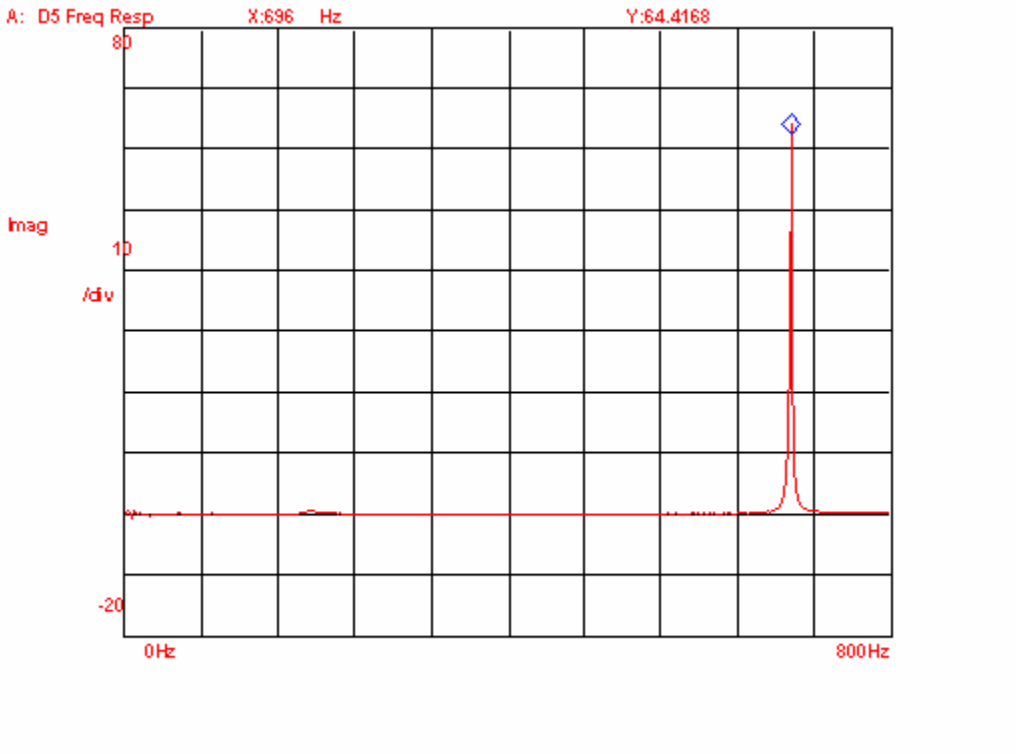

Fig. 27: FRF due to an impact at the node of the first mode

Table 8: Modal test results for aluminum bat

	Frequencies (Hz)	Node points close to sweet spot (in)
First mode	198	6.69
Second mode	696	5.00
Third mode	1412	3.94

The mode shapes from experimental results and FEA models were also compared for the calibration of the FEA model. Fig. 28 shows the mode shapes from experimental and FEA values. It is seen from Fig. 28 that there is good correlation between experimental and FEA values.

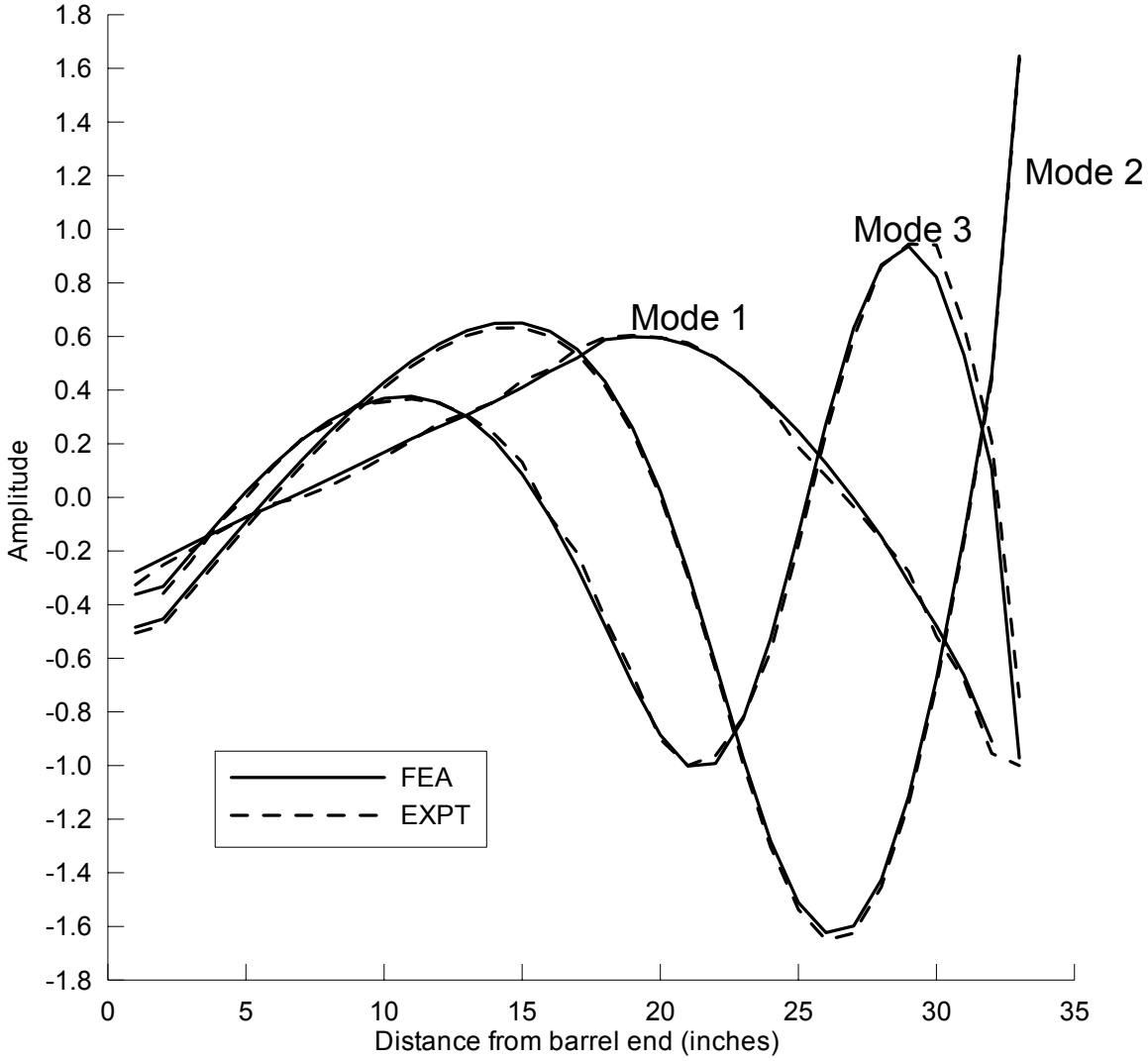

Fig. 28: Comparison of FEA and experimental mode shapes of aluminum bat

6.2.2 Aluminum Bat Performance

The bat performance was measured experimentally using the BHM and analytically using the finite element method. After all the experimental calculations were done, a performance curve was drawn for the aluminum bat with the recorded values. The performance curve was drawn with the ball exit velocity on the y-axis and location of impact on the x-axis. Sweet spot, COP and node points are also marked in this plot. Fig.

29 shows the performance curve for the aluminum bat used in this thesis. This performance curve was drawn with experimental values. Fig. 29 shows that the performance of the bat varies parabolically along the length of the barrel. The peak location is the sweet spot, which in this case is 6.0 in. from the tip of the barrel. The trend line shown in the figure is a parabolic curve fit of the experimental data. Fig. 29 also shows that the sweet spot lies between the nodes of the first two bending modes and the COP.

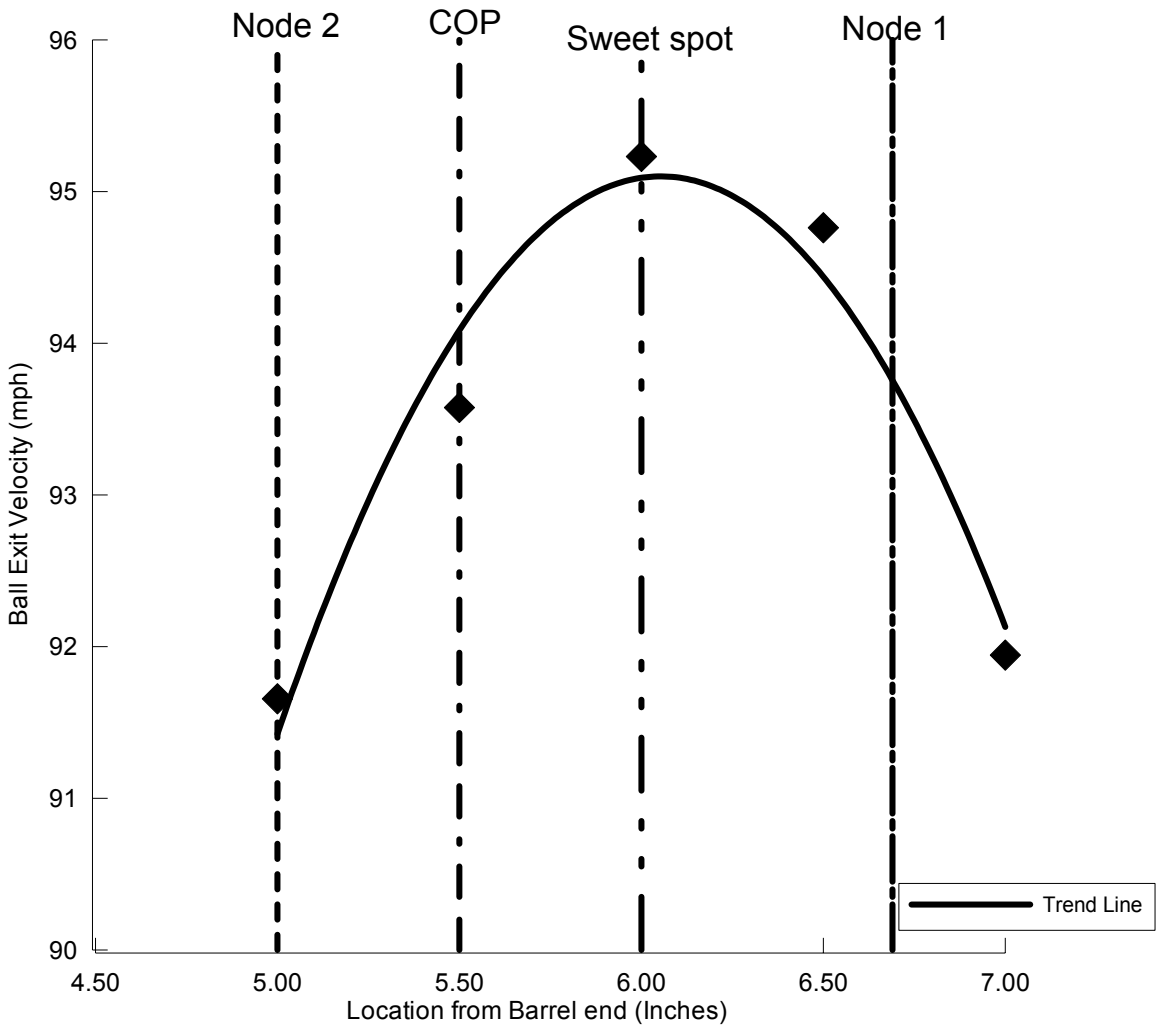

Fig. 29: Performance curve for aluminum bat - experimental values

6.2.3 Wood Bat

Figs. 30 and 31 show the FRFs of the wood bat. These FRFs are obtained by impacting the bat along the grains.

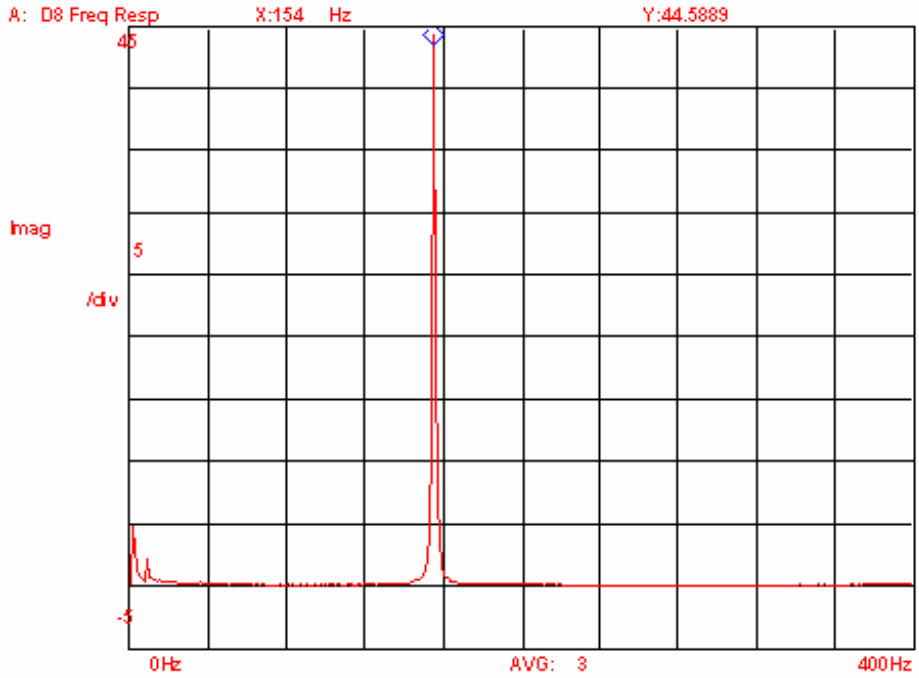

Fig. 30: Wood bat - first bending mode

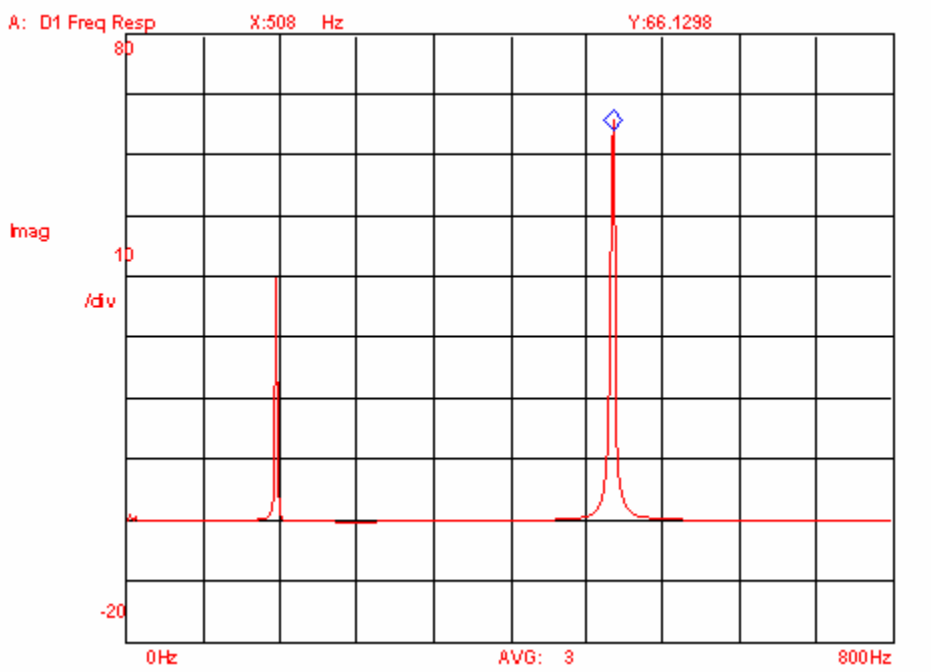

Fig. 31: Wood bat - second bending mode

The mode shape plots of the wood bat, which were plotted by recording the amplitudes at every inch on the bat, are shown in Figs. 32 and 33. The FRF for the nodal impact (node close to the sweet spot only) on the wood bat is shown in Fig. 34.

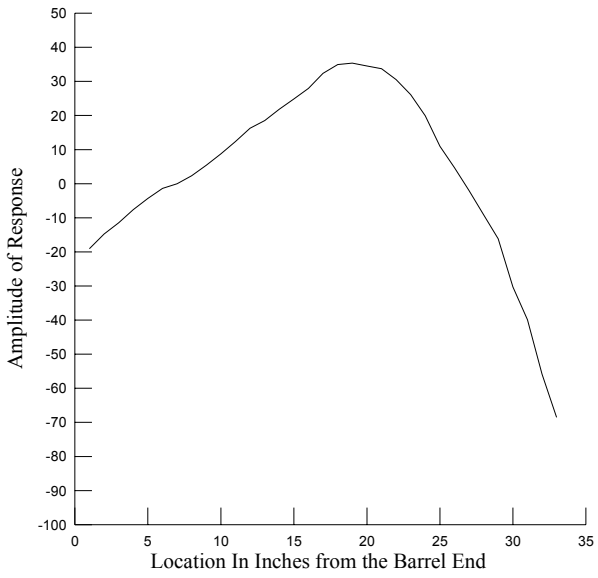

Fig. 32: Wood bat first mode shape plot - experimental

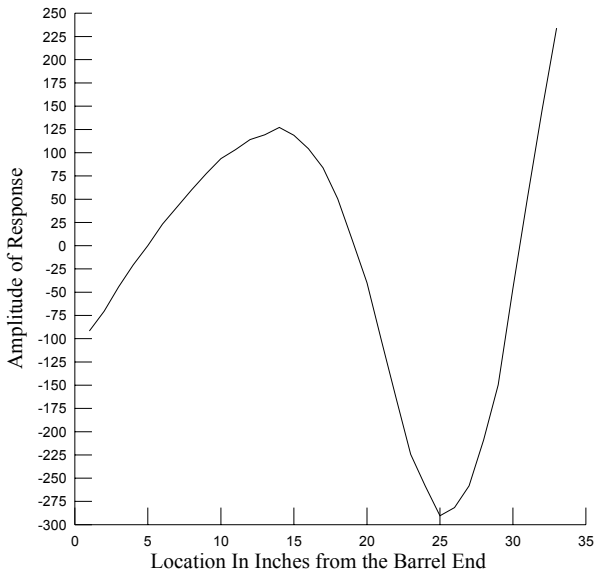

Fig. 33: Wood bat second mode shape plot – experimental

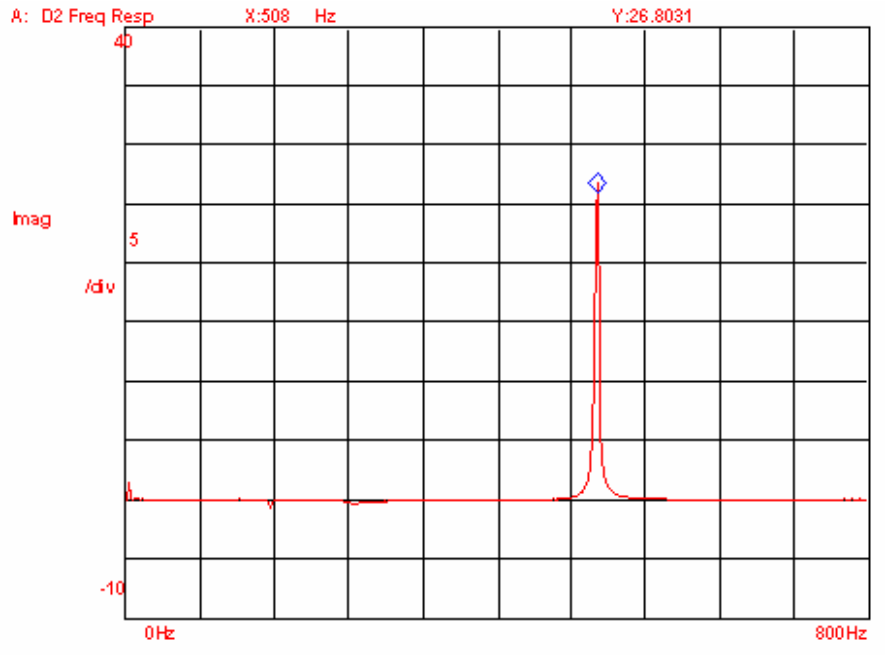

Fig. 34: FRF due to an impact at the node of the first mode of wood bat

All the above measurements on the wood bat were made by impacting the bat along the grains. The wood bat was rotated 90° to impact perpendicular to the grains. The frequencies decreased when impacted perpendicular to the grain. As the bat is tested by impacting it along the grains in the BHM, the frequencies recorded by impacting the bat along its grains were used for this research to maintain consistency. Fig. 35 shows the FRF of the wood bat obtained by impacting it perpendicular to the grains. Table 9 shows the results of the modal test on wood bat. Fig. 36 shows the comparison of experimental vs. FEA modes shapes of the wood bat.

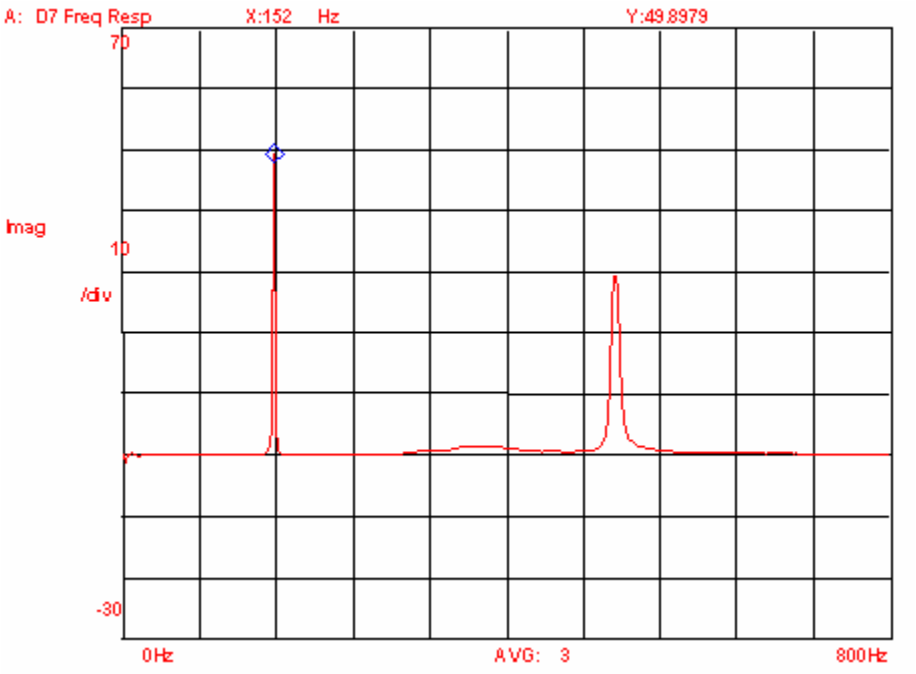

Fig. 35: FRF of a wood bat due to an impact perpendicular to grains

Table 9: Modal test results for wood bat

	Frequencies (Hz)		Node points close to sweet spot (in)
	along grains	perpendicular to grains	
First mode	154	152	6.56
Second mode	508	506	4.94
Third mode	1008	1003	3.94

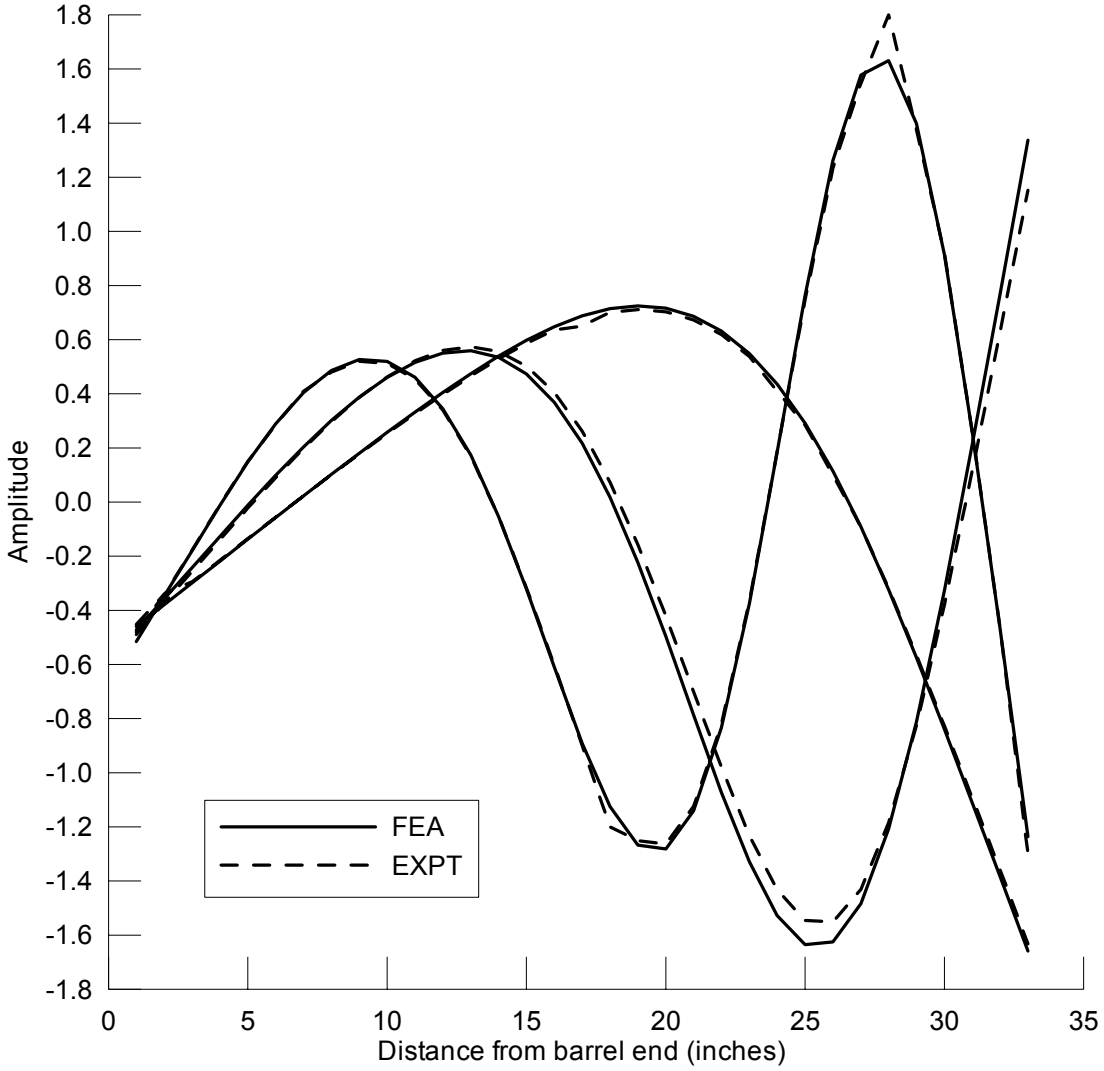

Fig. 36: Comparison of Experimental vs. FEA mode shapes of the wood bat

6.2.4 Wood Bat Performance

The performance curve for the wood bat along with the sweet spot, COP and node points is shown in Fig. 37. The performance curves for the wood bat and the aluminum bat are similar in shape. The sweet spot, as shown in Fig. 37, lies between the two node points and the COP. In addition, the curve is plotted only at three locations as the BHM test is halted once the sweet spot is identified which in this case is at 6.5 in. from the tip of the barrel.

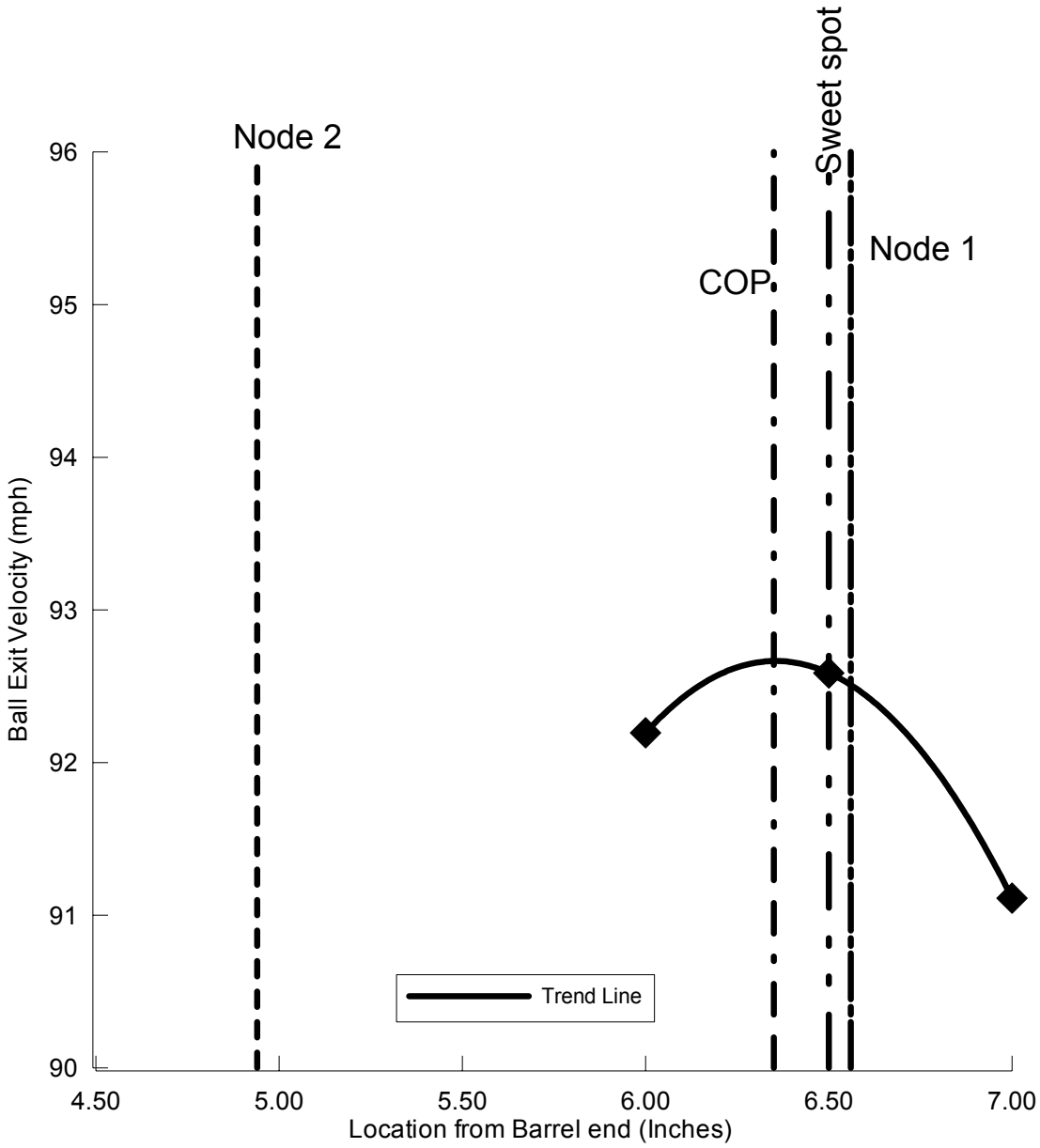

Fig. 37: Performance curve for wood bat – experimental

6.2.5 Ball

The COR of the ball was measured by pitching the ball at different speeds. The test was repeated with two balls to check for consistency. The speeds and the corresponding COR are listed in Table 10. Fig. 38 shows a plot of COR of the ball vs. pitched speed. Table 10 and Fig. 38 show that the COR of the ball decreases with increasing pitch speed.

Table 10: Ball COR vs. pitch speed

Ball 1		Ball 2	
Input (mph)	COR	Input (mph)	COR
40.394	0.571	38.674	0.560
49.652	0.547	50.000	0.539
59.106	0.536	58.341	0.530
70.462	0.525	71.280	0.515
85.644	0.508	82.629	0.507
97.076	0.492	95.409	0.488
100.591	0.490	97.235	0.487
102.985	0.483	101.727	0.482

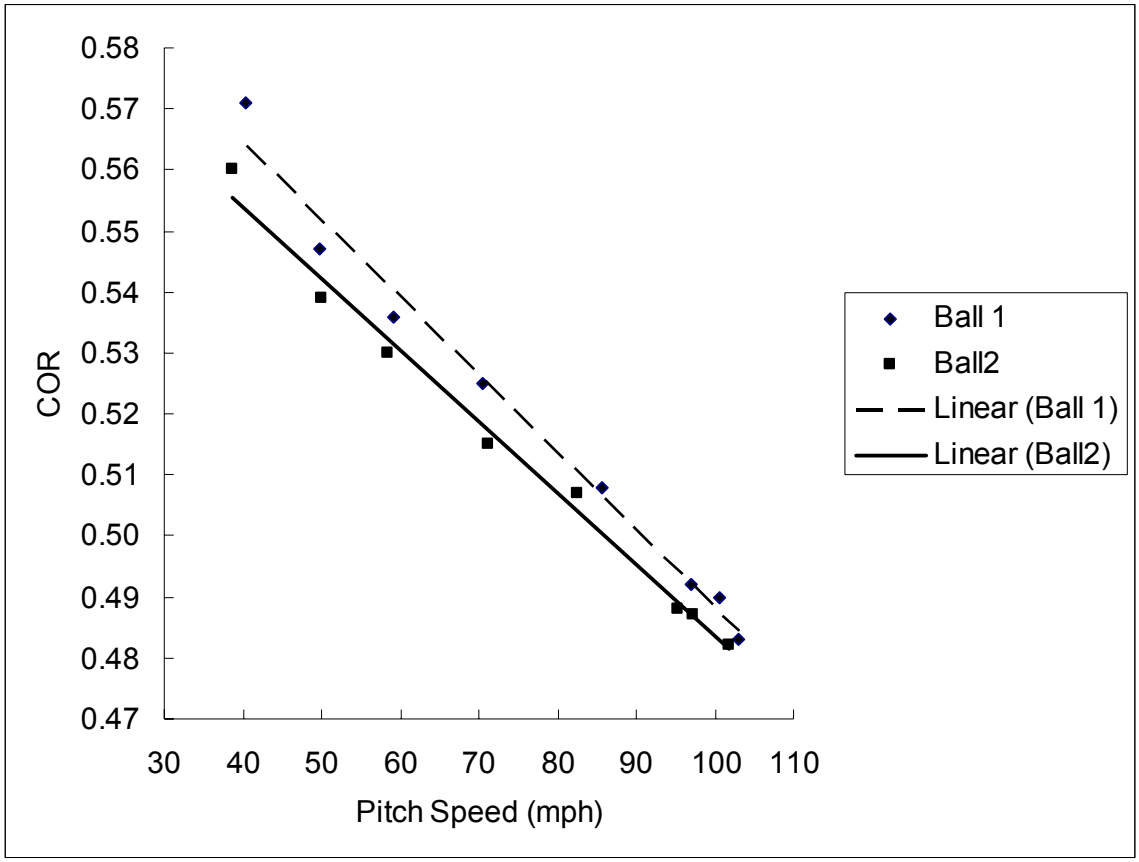

Fig. 38: Ball COR vs. pitch speed – experimental

6.3 FINITE ELEMENT MODELING RESULTS

Results obtained from finite element models of wood and aluminum bats and the baseball are presented in this section. Results from the models are compared with experimental values for calibration.

6.3.1 Aluminum Bat

In this research, three different models of the aluminum bat were made during the process of calibration of the models to experimental values. Results are presented in this section.

The first model was an aluminum bat made with only two components, the bat and the end cap (Model 1). The bat was made with a uniform thickness of 0.100 in. The mass, MOI, CG and COP of this model are listed in Table 11. An eigen-analysis of the bat was also done to extract the frequencies, mode shapes and the nodal locations. These values are listed in Table 11 along with the experimental values.

Table 11: Results from FEA Model 1 (two components only)

Method	Mass	MOI @ knob	CG	Node 1	Node 2	COP	Sweet spot	Mode 1	Mode 2
(units)	(oz)	(oz-in^2)	(in)	(in)	(in)	(in)	(in)	(Hz)	(Hz)
Exp	30.695	16147	12.50	6.69	5.00	5.50	6.00	198	696
FEA	30.695	14864	12.29	7.36	5.50	6.12	6.50	213	719

All the position values (Node 1, Node 2, COP and Sweet spot) in Table 11 were measured from the tip of the barrel of the bat. Table 11 shows a significant difference between the finite element model and the experimental values. The difference in mass

distribution between the real bat and the model and variation in the wall thickness of the bat can cause the significant difference between the two.

A new model with four components, i.e. barrel, throat, handle and end cap was built. The thickness of each component was the average value of the thickness measured at every inch on the barrel, throat and handle on the actual bat (Model 2). Table 12 shows the results from this model.

Table 12: Results from FEA Model 2 (four components)

Method	Mass	MOI @ knob	CG	Node 1	Node 2	COP	Sweet spot	Mode 1	Mode 2
(units)	(oz)	(oz-in^2)	(in)	(in)	(in)	(in)	(in)	(Hz)	(Hz)
Exp	30.695	16147	12.50	6.69	5.00	5.50	6.00	198	696
FEA	30.695	15487	12.61	7.25	5.25	6.38	6.00	199	710

Table 12 shows that Model 2 correlated better with the experimental values than did Model 1. The frequencies were very close to the experimental values. However, there were still some differences in the MOI, CG and frequency values.

The model was further refined by using the actual thickness values at every inch along the length of the bat. This new model (Model 3) had 34 components (33 for the bat + 1 for the end cap). Results from Model 3 are presented in Table 13. Model 3 gave the best agreement between the model and all of the parameters (MOI, CG, Node 1, Node 2 COP, Sweet spot, Mode 1 and Mode 2) and the corresponding experimental values.

Table 13: Results from FEA Model 3 (34 components)

Method	Mass	MOI @ knob	CG	Node 1	Node 2	COP	Sweet spot	Mode 1	Mode 2
(units)	(oz)	(oz-in^2)	(in)	(in)	(in)	(in)	(in)	(Hz)	(Hz)
Exp	30.695	16147	12.50	6.69	5.00	5.50	6.00	198	696
FEA	30.696	16163	12.00	7.00	5.25	6.53	6.00	198	711

6.3.2 Wood Bat

The mass, MOI, CG, COP and natural frequencies of the wood bat were measured experimentally. The FEA model of the wood bat was then built, and the material properties used in the model were tuned to calibrate the model to the corresponding experimental values of the wood bat.

An eigen-analysis of the bat was done to compare the dynamics of the model to the experimental values. Results of the experimental calculations and FEA model of the wood are listed in Table 14.

Table 14: Comparison between experimental and FEA results of the wood bat

Method	Mass	MOI @ knob	CG	Node 1	Node 2	COP	Sweet spot	Mode 1	Mode 2
(units)	(oz)	(oz-in$^{2)}$	(in)	(in)	(in)	(in)	(in)	(Hz)	(Hz)
Exp	30.735	17369	10.88	6.56	4.94	6.35	6.50	154	508
FEA	30.732	17291	10.94	6.75	4.75	6.39	6.50	156	510

6.3.3 Mode Shapes

Figs. 39 through 45 show the FEA mode shapes of the wood and aluminum baseball bats. The hoop or breathing mode of the aluminum bat is also shown. The first three bending modes of the wood and aluminum and also the first breathing mode of the aluminum bat are shown.

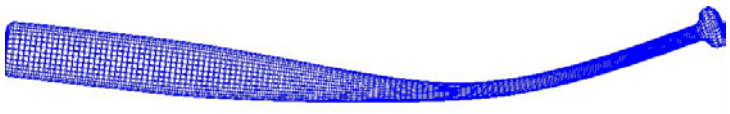

Fig. 39: Aluminum Mode 1

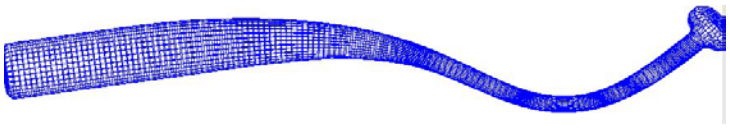

Fig. 40: Aluminum Mode 2

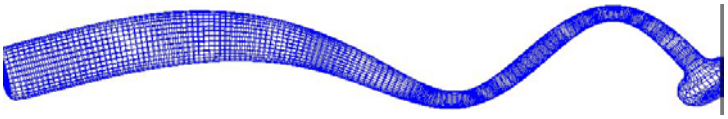

Fig. 41: Aluminum Mode 3

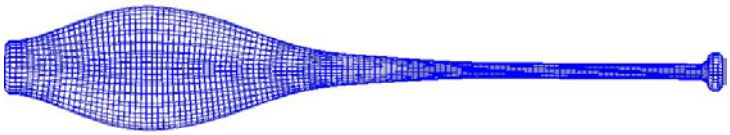

Fig. 42: Aluminum Hoop or Breathing Mode

Fig. 43: Wood Mode 1

Fig. 44: Wood Mode 2

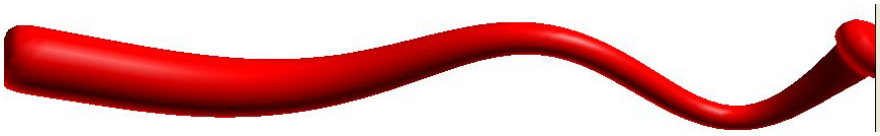

Fig. 45: Wood Mode 3

6.3.4 Ball Model

An FEA model of the ball was built, and the COR of the model was tuned to the experimental value for calibration. The ball model was calibrated such that the COR lies in the experimental range of the two balls tested. Fig. 46 shows the COR vs. Pitch Speed plots for both experimental values and FEA values. The solid lines are linear regressions of the data.

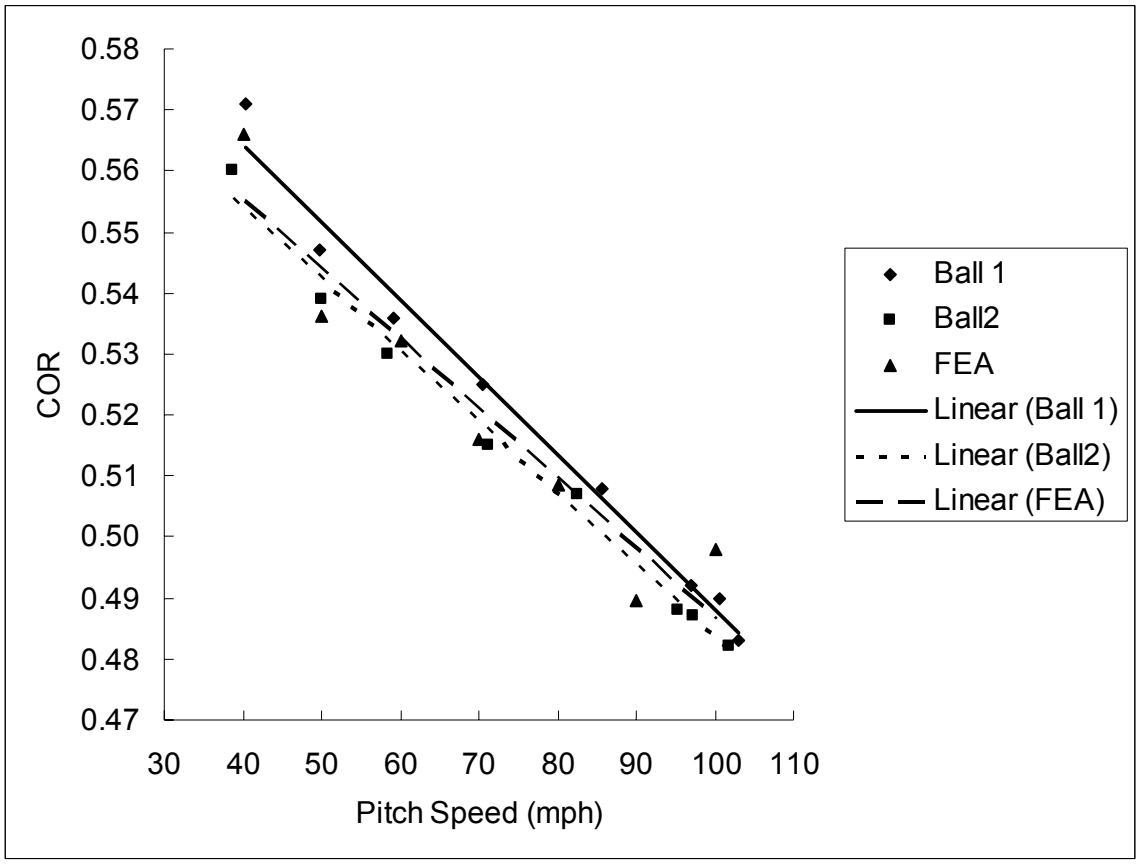

Fig. 46: COR vs. pitch speed - FEA Results

6.3.5 Finite Element Results for the Bat/Ball Impact

Contact between the bat and the ball was modeled by pitching the ball at 70 mph. The swing speed for the experimental bat-ball impact was 66 mph. However, swing speed varies with MOI and to accommodate the MOI differences between the FEA and Experimental values, the swing speed for bat-ball impacts of the FEA models were calculated using Eq. 5 (Section 3.2.2). Results from the finite element analyses of the aluminum and wood bats are listed in Tables 15 and 16, respectively. Tables 15 and 16 also show the experimental values. Figs. 47 and 48 show the performance curves for the FEA models of the wood and aluminum bats.

Table 15: Experimental and FEA values of ball exit velocities of aluminum bat

Location (in)	Experiment (mph) [Swing speed 66.0 mph]	FEA (mph) [Swing speed 65.98 mph]
5.0	91.656	95.164
5.5	93.576	96.491
6.0	95.231	96.924
6.5	94.761	96.646
7.0	91.944	95.563

Table 16: Experimental and FEA values of ball exit Velocities of wood bat

Location (in)	Experiment (mph) [Swing speed 66.00 mph]	FEA (mph) [Swing speed 66.09 mph]
5.0	N/A	92.567
5.5	N/A	92.964
6.0	92.195	93.012
6.5	92.587	93.610
7.0	91.112	91.614

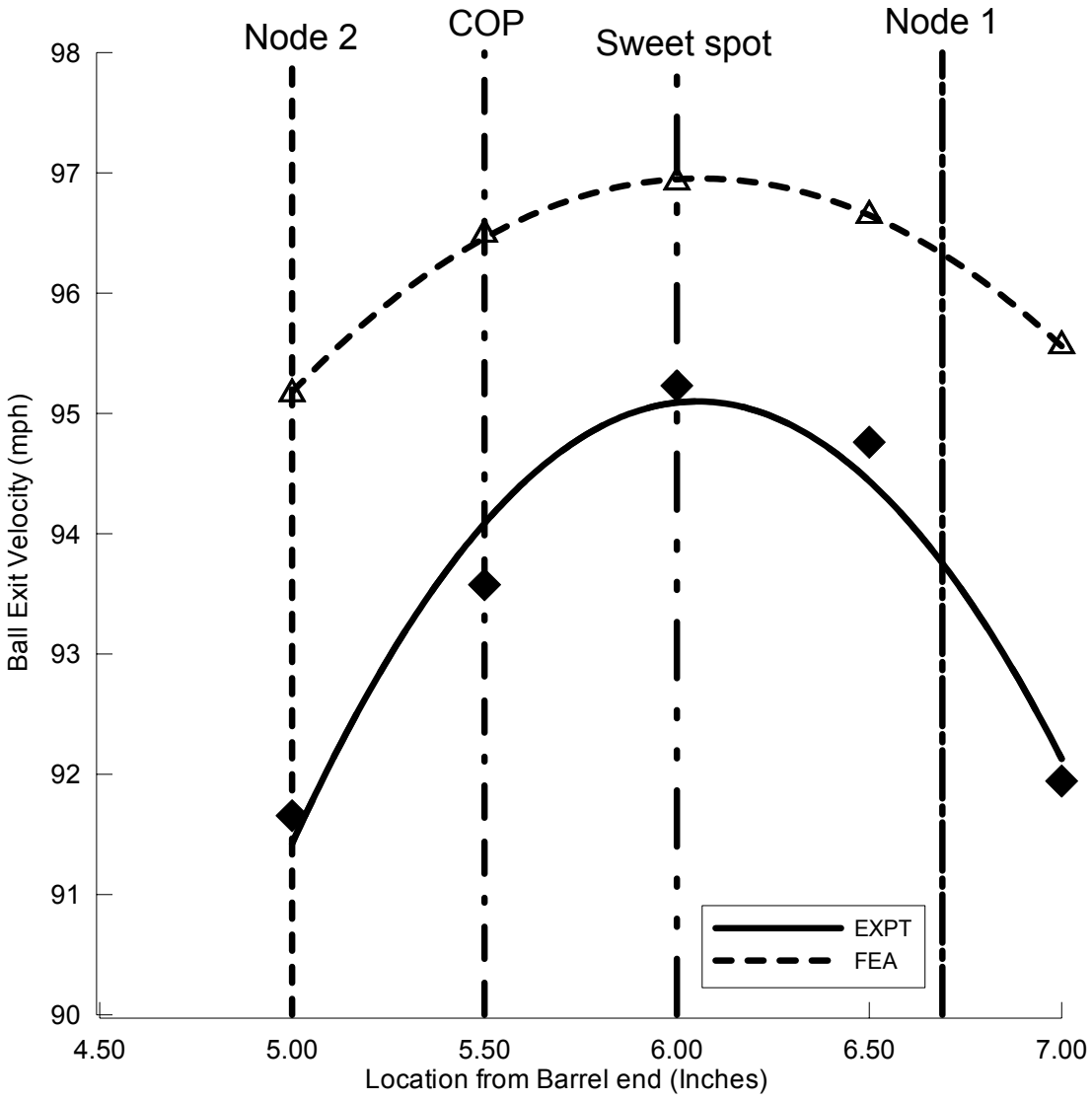

Fig. 47: Performance curves for the FEA and experimental values of the aluminum bat

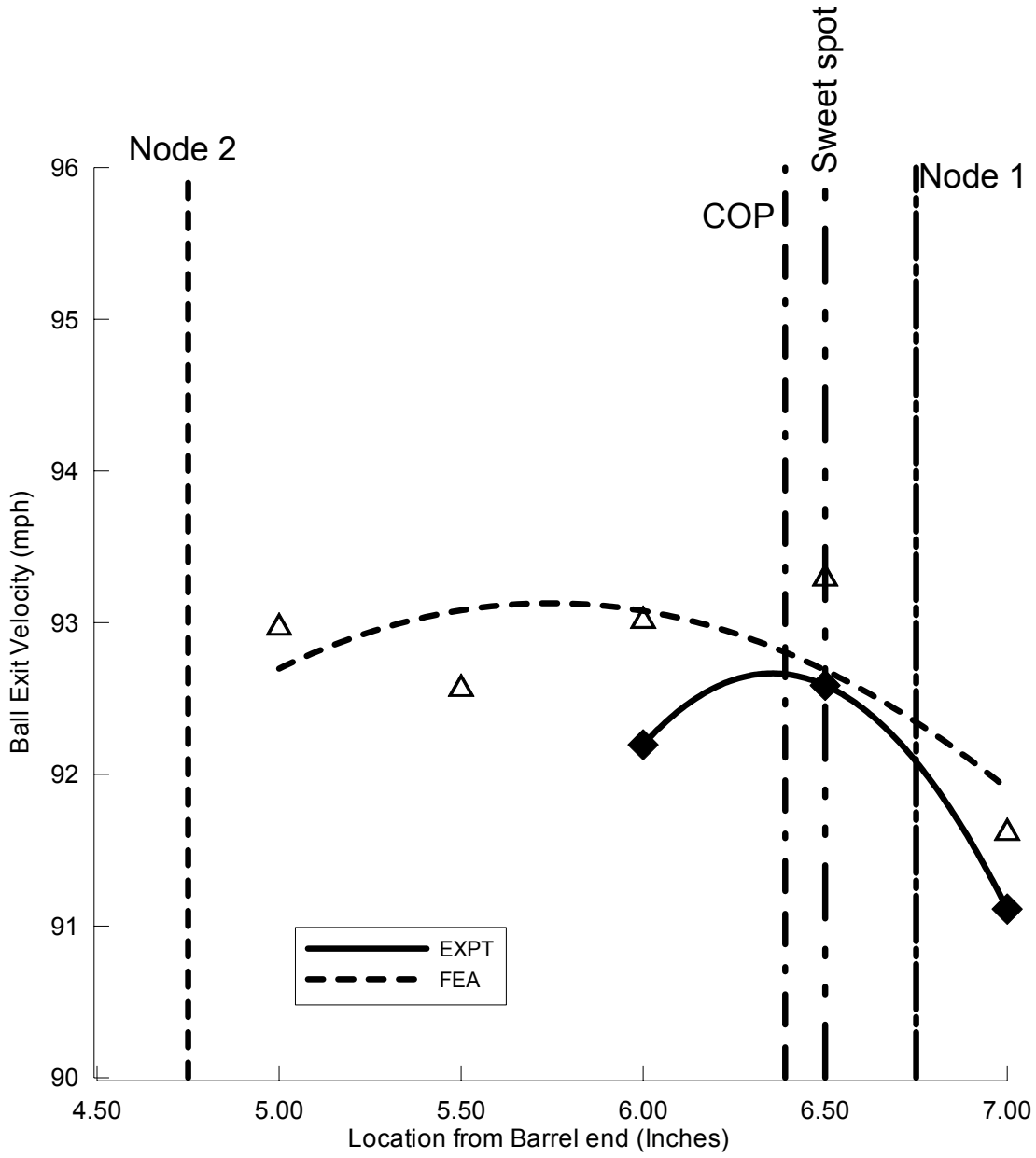

Fig. 48: Performance curves for the FEA and experimental values of the wood bat

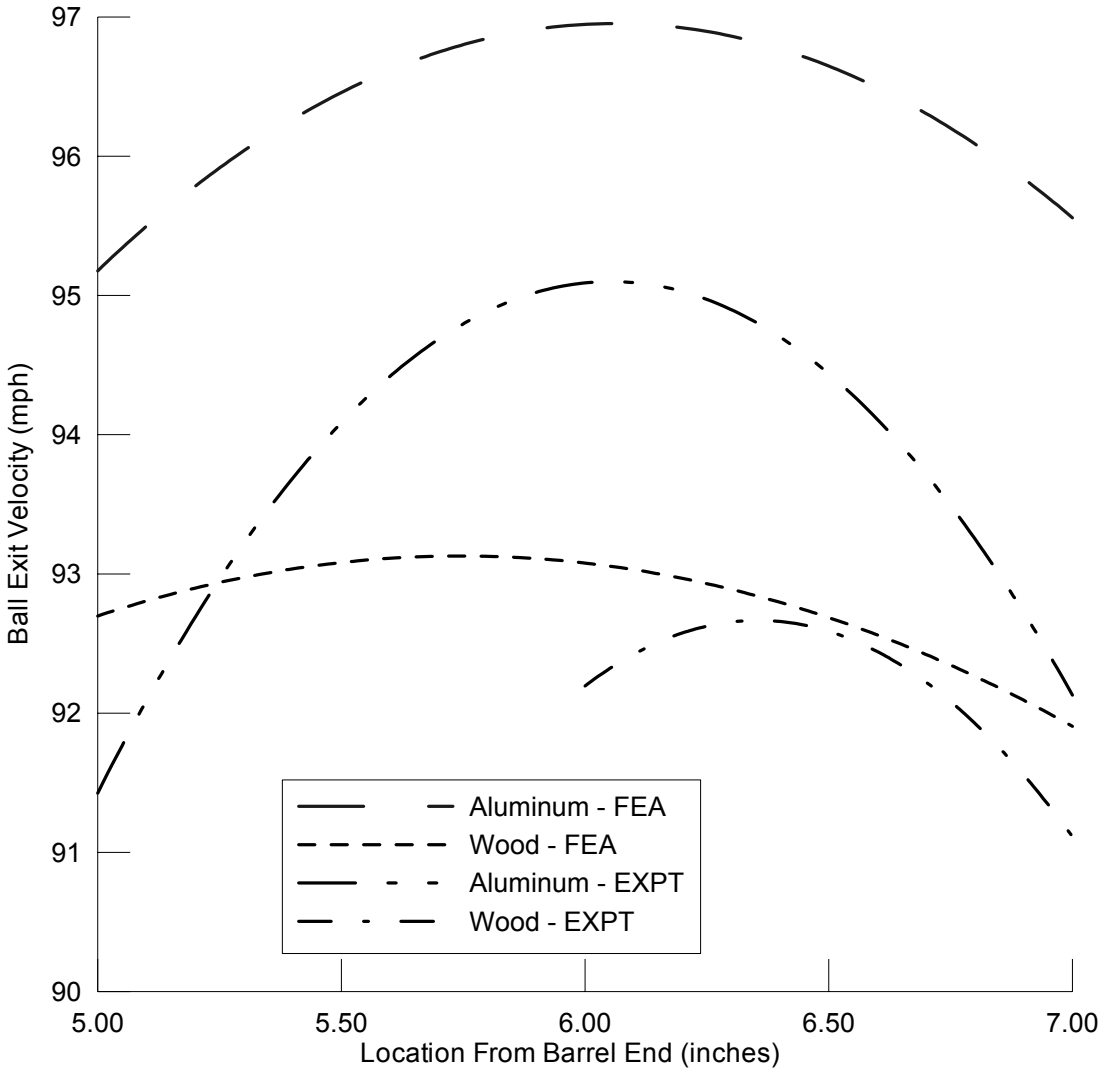

Fig. 49: Performance summary

Fig. 49 shows the summary of the performance of the two bats. Fig. 49 shows that the FEA models predict higher than the experimental performance of the bats. This may be because of the differences in geometry, material properties, and/or mass distribution between the actual bats and the FEA models and also the amount of damping present in the bats which is not properly quantified in the models.

6.4 Results From Parametric Study

To understand how various design parameters can affect bat performance, the inertial and vibrational properties of the bats were changed, and their effects on the performance of the bats were studied. The results of these parametric studies are covered in this section. The properties of the bats are changed and the corresponding change in frequencies, location of sweet spots, node point and COPs are tracked along with the change in swing speeds (due to change in MOI), change in contact time and hence the change in ball exit speeds.

6.4.1 Change in Mass of the Bat

To study the influence of mass on the performance of bat, the mass of the aluminum bat was doubled and the resulting change in performance was recorded. The bat swing speed, ball mass and ball pitch speed were kept constant for this study. These results are shown in Table 17. It is seen from Table 17 that doubling the mass of the bat, increased the ball exit velocity by 17 mph. This increase in ball exit velocity was because more mass brings in more initial momentum into collision.

Table 17: Mass vs. ball exit velocity as a function of bat mass

Method	Mass (oz)	Bat swing speed (mph)	Ball exit velocity BEV (mph)
Initial	30.696	65.9	96.15
Doubled	61.392	65.9	113.10

6.4.2 Change in Bat Swing Speed

The affect of bat swing speed on the performance was studied by doubling the bat swing speed and recording the resulting ball exit velocities. The results are shown in Table 18. It is seen in these results that doubling the bat swing speed, increases the ball exit speed by 78 mph. Comparing the results from doubling the mass to doubling the swing speed models, it is observed that it is advantageous to swing the bat at a higher speed rather than to swing a heavier bat at the same velocity.

Table 18: Bat swing speed vs. ball exit velocity

Method	Mass (oz)	Bat swing speed (mph)	Ball exit velocity BEV (mph)
Initial	30.696	65.9	96.15
Doubled	30.696	131.9	174.11

6.4.3 Change in Moment of Inertia

The moment of inertia of the bat was varied, and its effect on the performance of the bat was measured. The moment of inertia of the bat was varied by decreasing the overall thickness of the bat by 10% and adding additional mass either at the barrel end (barrel loaded) or at the knob end (knob loaded) to keep the overall mass of the bat constant. The additional mass was added by increasing the mass density. The results from these models are shown in Table 19. Table 19 shows the results with a bat swing speed that was calculated using Eq. 5 (Section 3.2.2) at 6.0 in. from the tip of the barrel. It is seen in Table 19 that as the swing speed increases, the ball exit velocity also increases. The contact time for the bat and ball decreased with increasing swing speed. The change in swing speed with change in MOI was also plotted to study the trend. It is seen in Fig. 50 that as the MOI increases the swing speed of the bat decreases.

Table 19: MOI change results

Method	Mass (oz)	MOI@knob (oz-in^2)	CG (in)	Swing speed (mph)	BEV (mph)
Barrel loaded	30.696	16287	11.90	65.832	96.62
Original	30.696	16163	12.00	65.981	96.15
knob loaded	30.696	15950	12.28	66.237	95.38

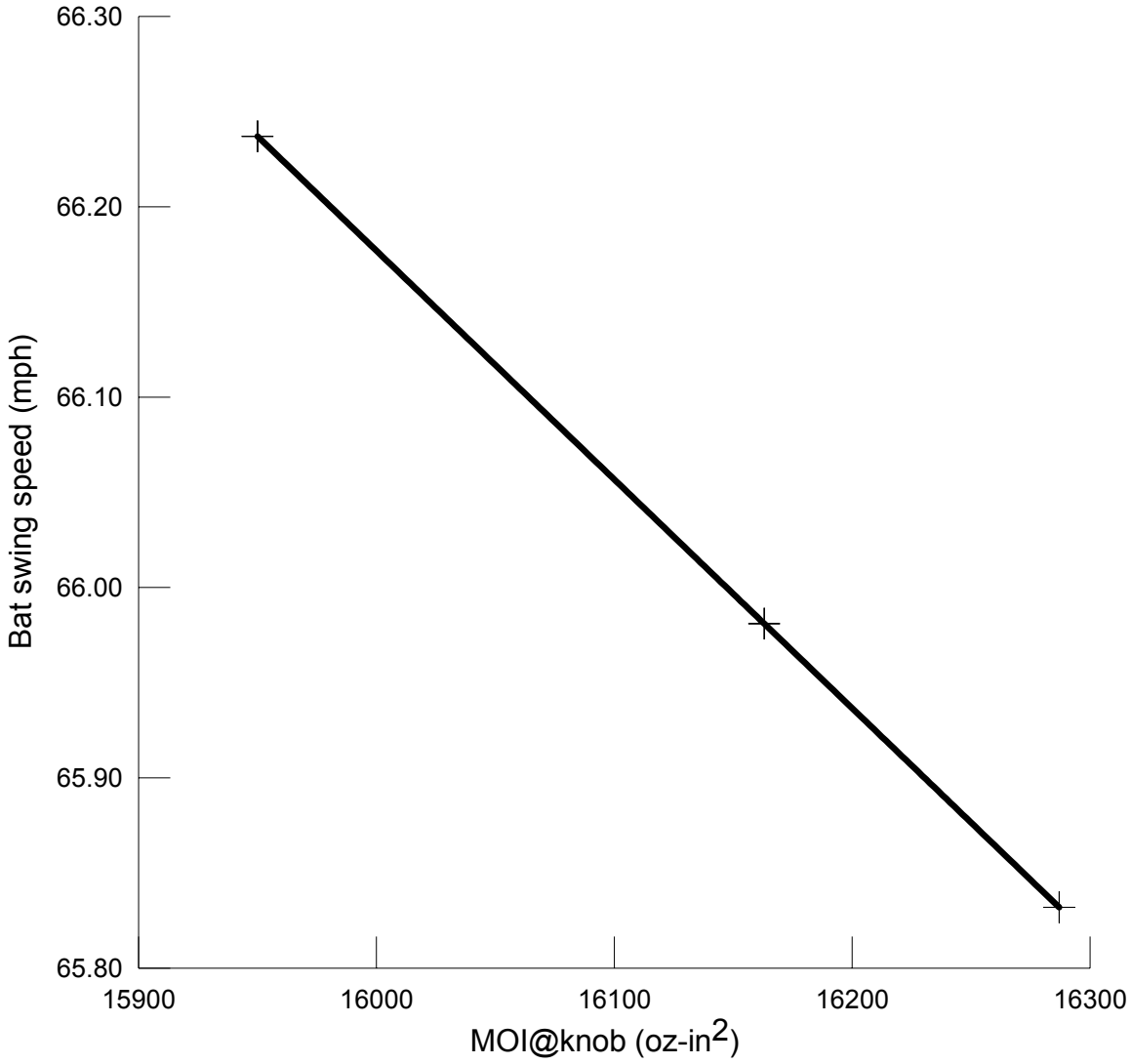

Fig. 50: MOI vs. bat swing speed

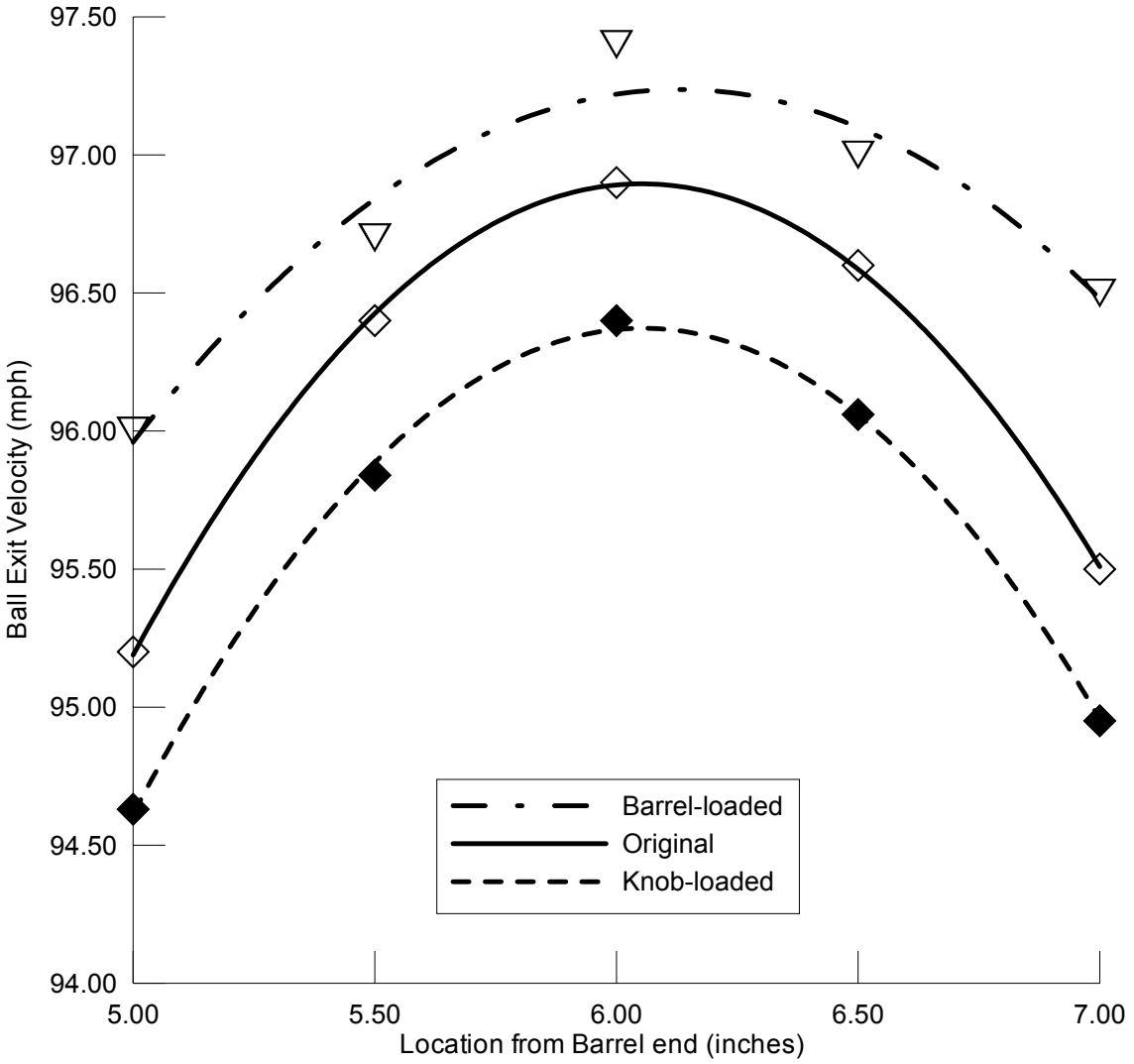

Fig. 51: Performance vs. MOI change

Fig. 51 shows the performance curves for the original, knob-loaded and barrel-loaded models. The barrel-loaded model is observed to produce the greatest exit velocity. This result is expected because this configuration has the greatest concentration of mass in the vicinity of the impact.

6.4.4 Change in Stiffness

The stiffness of the aluminum bat was then changed to see how it affects the COP and the node points. The stiffness of the model was altered by changing only the elastic modulus of the material. The frequencies were increased with the increase in modulus, but there was no change in the locations of the COP, CG, nodes or sweet spot. However, for a 10% increase in modulus, the ball exit velocity decreased by 0.6%. Table 20 shows the ball exit velocities with respect to change in stiffness. Fig. 52 shows the performance curves. Fig. 53 shows that the contact time is also decreasing with increasing stiffness and vice versa. As the contact time decreases, the amount of energy that is imparted to the ball also decreases and hence there is a decrease in performance.

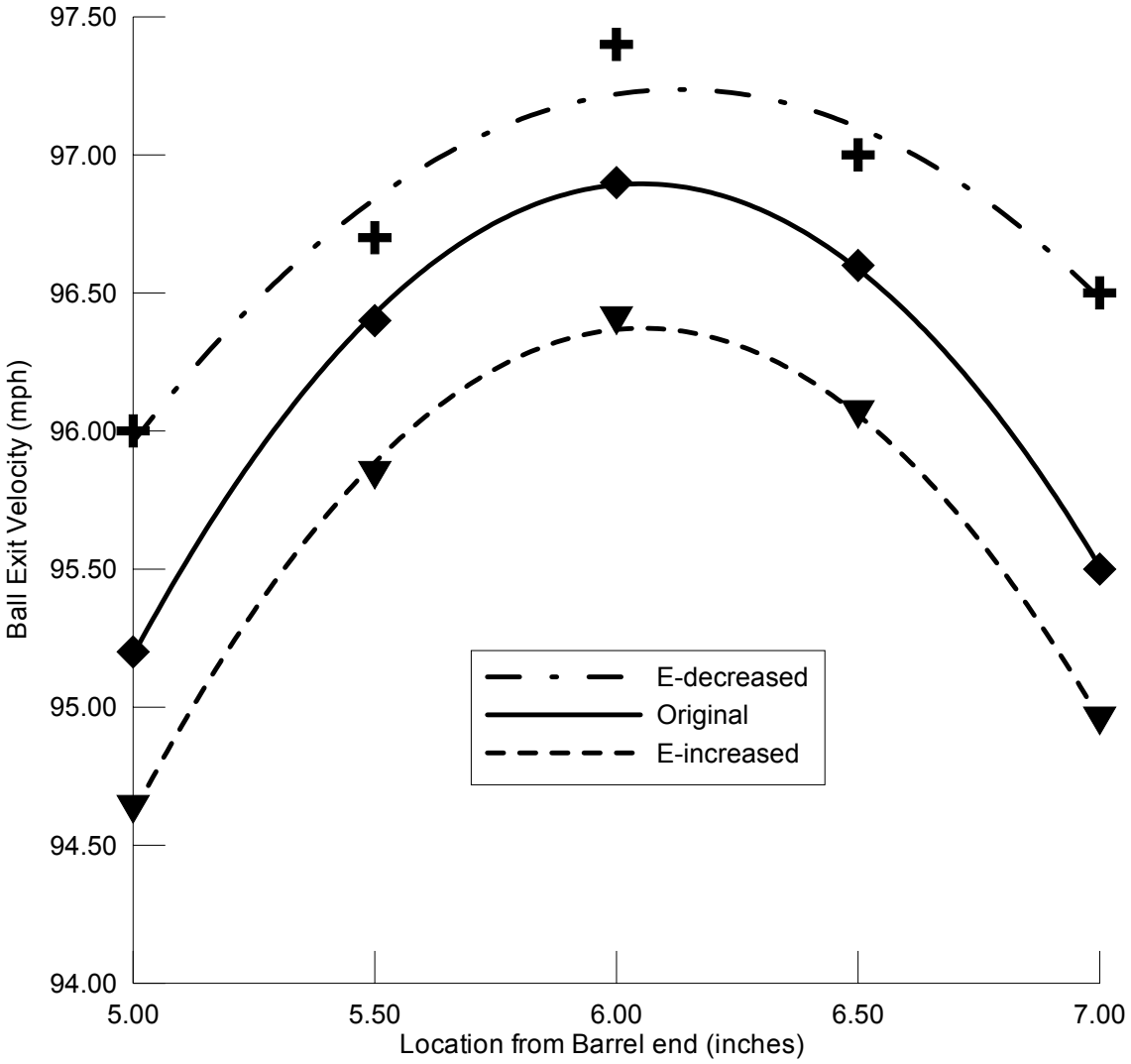

Fig. 52: Performance vs. change in stiffness

Table 20: Ball exit velocities vs. stiffness

Method	Mass (oz)	Young's Modulus (Mpsi)	BEV (mph)
E-Increased	30.696	12.00	95.58
Original	30.696	11.14	96.15
E-Decreased	30.696	10.56	96.72

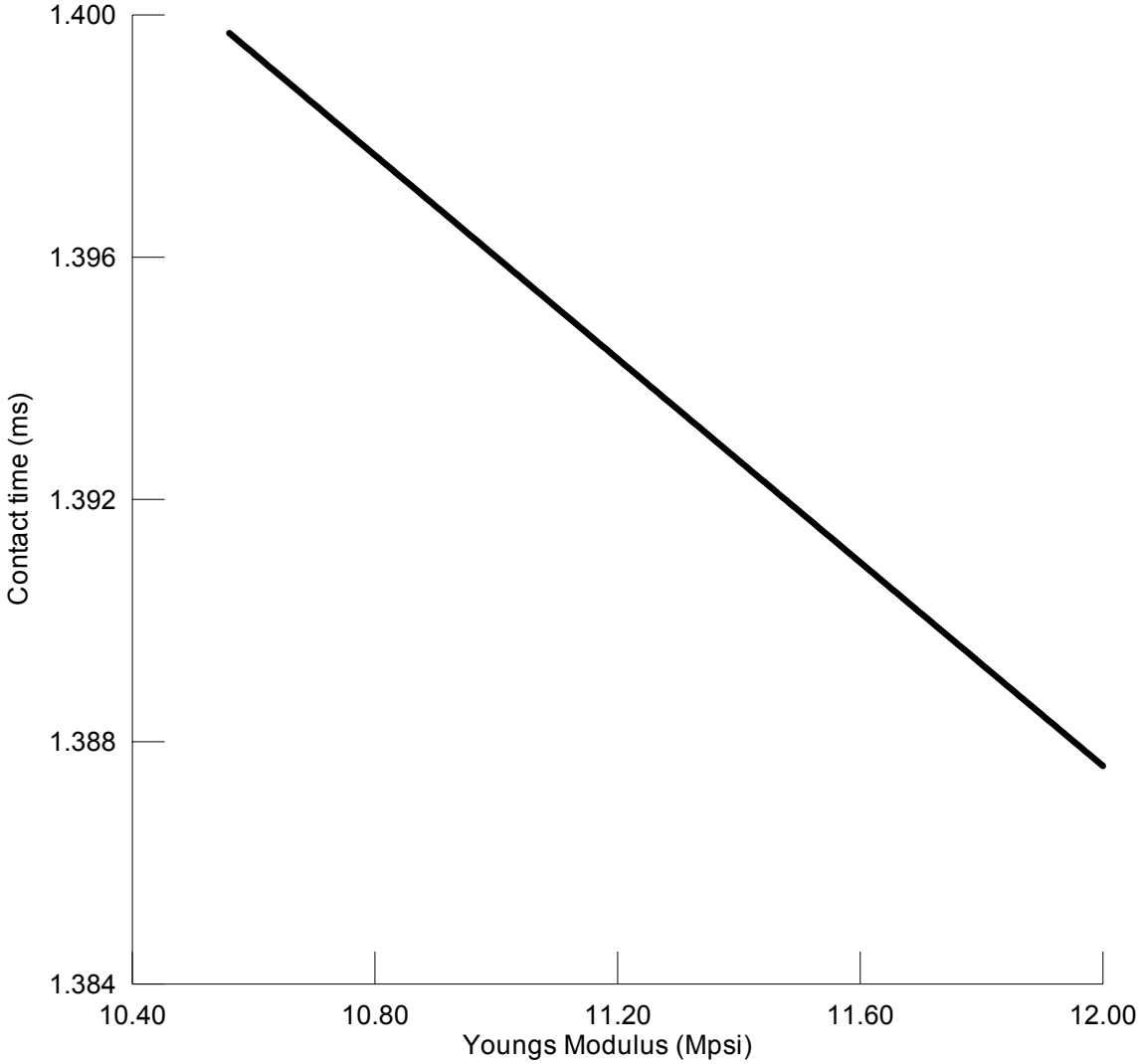

Fig. 53: Stiffness vs. contact time

6.4.5 Change in Wall Thickness of the Bat

The effect of wall thickness on the performance of the bat was studied by changing the thickness of the bat. The overall thickness of the bat and the thickness of each of the barrel, throat and handle were changed and the mass density was adjusted such that the overall mass of the bat remained the same. Table 21 shows the wall-thickness-change results with the different models. The percentage shown in the Table 21 is the percentage change in the thickness relative to the original bat model. The performance of the bat looked to be decreasing with increasing wall thickness. This is because in the case of a thickness change in the whole bat and barrel sections, decreasing the thickness decreases the MOI@knob and hence increases the swing speed. However, in the case of a thickness change in the throat and the handle, there is more mass in the barrel region which therefore gives a higher ball exit velocity.

Table 21: Results of thickness-change models

Method	Mass (oz)	MOI@knob (oz-in^2)	CG (in)	Swing speed (mph)	BEV (mph)
Original	30.696	16163	12.00	65.981	96.15
Whole bat 10% decreased	30.694	16165	12.00	65.979	96.37
Whole bat 10% increased	30.695	16167	12.00	65.976	95.96
Barrel 10% decreased	30.696	16128	12.03	66.023	96.35
Barrel 10% increased	30.696	16207	11.97	65.928	95.81
Throat 10% decreased	30.696	16174	11.99	65.968	96.18
Throat 10% increased	30.696	16151	12.02	65.996	95.94
Handle 10% decreased	30.696	16195	11.97	65.943	96.22
Handle 10% increased	30.696	16157	12.01	65.988	96.01

6.4.6 Effect of Hoop Frequencies of the Bat

From the thickness change models, it is also observed that an increase in the hoop mode or breathing mode frequency decreases the bat performance. This decrease in performance is because an increase in the thickness decreases the trampoline effect of the aluminum bat. Thus, the ball deforms more as the wall thickness increases. This increased ball deformation results in less elastic energy being stored in the bat which can be returned to the ball. Also, increased ball deformation results in more energy being dissipated by the ball. This trampoline effect is further investigated by looking at hoop frequencies.

It is observed that frequencies vary linearly with change in thickness, and hoop frequencies seem to be changing significantly (when compared to bending frequencies) with change in the overall thickness of the bat as well as with change in the thickness of the barrel section alone. Tables 22 and 23 show changes in frequencies with changes in wall thickness of the bat. As seen from the Tables 22 and 23, the percentage changes in the hoop frequencies are greater than the percentage changes in the bending frequencies. Therefore, any changes in performance in relation to frequencies in these two models can be attributed largely to the hoop-frequency changes. It is therefore, inferred that increasing the hoop frequencies would decrease the performance of the bat provided there is less change in fundamental bending frequencies. This inverse pattern is expected as at lower hoop frequencies, the trampoline effect or barrel-breathing mode is excited, which will impart greater velocity to the ball.

Table 22: Thickness change in whole bat and barrel sections vs. frequencies

Frequencies (Hz)	Change in thickness				
	Original	Whole bat decreased 10%	Whole bat increased 10%	Barrel decreased 10%	Barrel increased 10%
First 3 Bending Frequencies	198	197	200	198	198
	711	707	712	711	711
	1410	1390	1411	1410	1410
First Hoop Frequency	2350	2288	2354	2328	2388
BEV (mph)	96.15	96.37	95.96	96.35	95.81

Table 23: Thickness change in throat and handle sections vs. frequencies

Frequencies (Hz)	Change in thickness				
	Original	Handle decreased 10%	Handle increased 10%	Throat decreased 10%	Throat increased 10%
First 3 Bending Frequencies	198	198	199	198	198
	711	709	711	710	712
	1410	1400	1410	1410	1410
First Hoop Frequency	2350	2350	2350	2350	2350
BEV (mph)	96.15	96.22	96.01	96.18	95.94

The changes in frequencies with changes in throat and handle thickness are shown in Table 23. It is seen from these results (Table 23) that changes in throat or handle thickness have no effect on the hoop frequencies.

The results in Tables 21 through 23 are only for 10% change in thickness. To study the effect of thickness on hoop frequencies and on the performance of the bat, the thickness of the whole bat was changed by ±20% and ±30% and the resulting change in performance and hoop frequencies was studied. Table 24 shows the results of these models. It can be concluded from Table 24 that performance decreases with increase in thickness and increase in hoop frequencies. The mass of all these models was kept the same by changing the density. Fig. 54 shows the effect of hoop frequencies on the performance of the bat. Data points in Fig. 54 were plotted using Table 24. The effect of thickness and hoop frequencies on the performance of the bat can be understood from Fig. 55. It is seen from Fig. 55 that as the thickness increases, hoop frequency increases and performance decreases.

Table 24: Effect of thickness and hoop frequencies on performance

Method	MOI @ knob ($oz\text{-}in^2$)	CG (in)	Swing speed (mph)	Hoop frequency (Hz)	Contact time (ms)	BEV (mph)
-30%	16117	12.033	66.036	1945	1.49997	102.58
-20%	16148	12.004	65.999	2053	1.49979	100.90
-10%	16166	12.000	65.978	2288	1.39997	96.37
Original	16163	12.000	65.981	2350	1.39988	96.15
+10%	16168	12.000	65.976	2354	1.39986	95.96
+20%	16295	11.852	65.823	2382	1.39996	93.85
+30%	16326	11.822	65.785	2449	1.39994	93.16

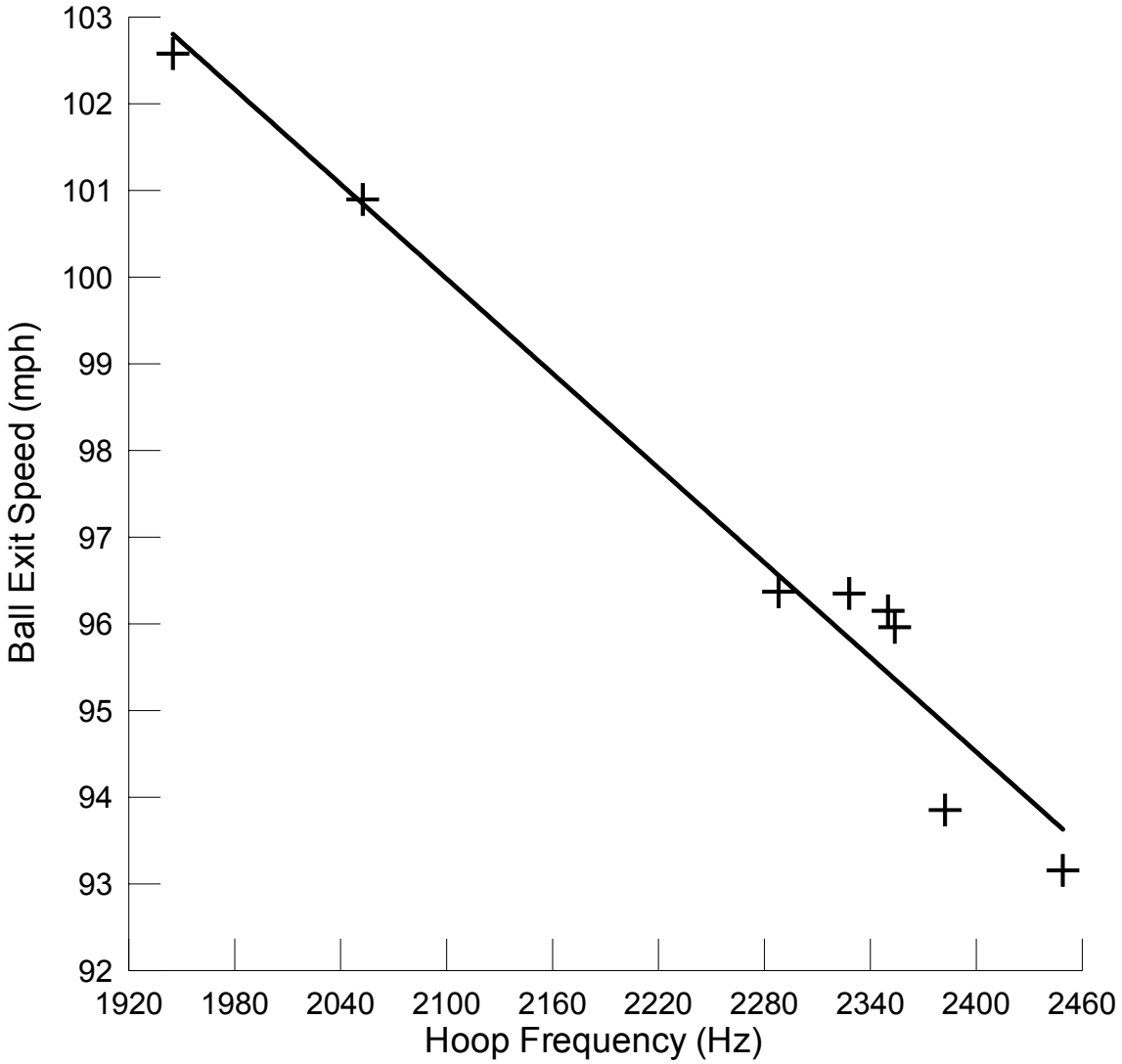

Fig. 54: Hoop Frequencies vs. performance

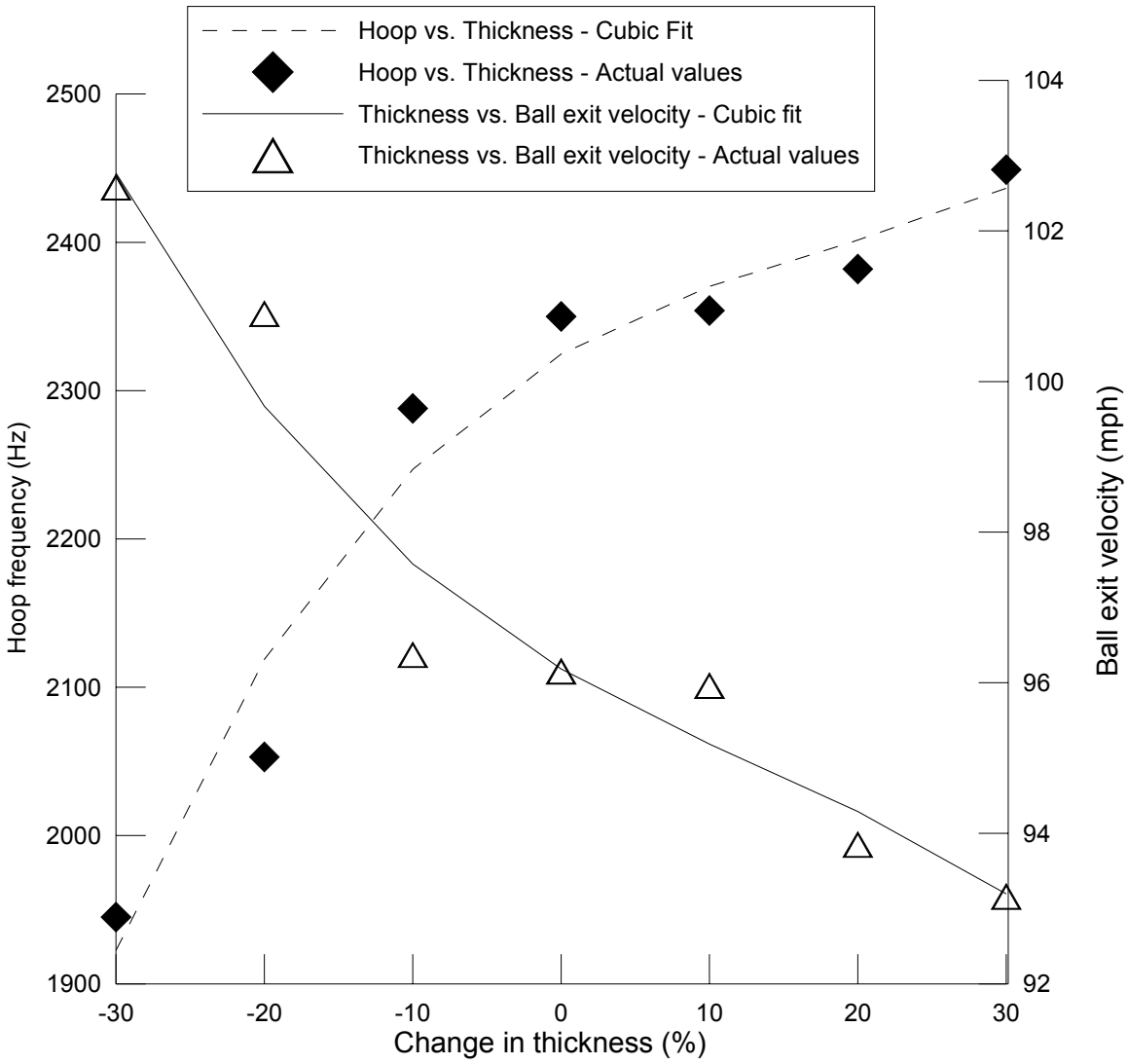

Fig. 55: Thickness vs. hoop frequency and ball exit velocity

6.4.7 COP, Node Points & Sweet Spot

After all the models were run, the results were analyzed to try to establish a relationship between the sweet spot, COP and node points. It was observed that impacts away from the node points produced lower ball exit speed when compared impacts close to node. Variations in COP, node points and sweet spot were observed but no quantitative relationship for their variation could be established. Table 25 shows that the sweet spots on these bats were between the nodes and the COP. All the measurements in Table 25 were recorded from the barrel end of the bat.

Table 25: Variation of sweet spot with COP and node points (experimental values)

Type	Sweet spot (in)	COP (in)	Node1 (in)	Node2 (in)
Aluminum	6.00	5.50	6.69	5.00
Wood	6.50	6.38	6.56	4.94

6.4.8 Wood Bat Parametric Study

The effect of different sizes of barrels and handles on the performance of wood bat was investigated by changing the bat model. It can be seen in Table 26 that bigger barrels and smaller handles produce the highest batted-ball speeds. This result is because there is more mass near the contact point in the case of bigger barrels. It is seen in Table 26 that an increase in swing speed increases the batted-ball speed.

Table 26: Wood bat parametric study results

Method	Mass (oz)	MOI @ knob (oz-in^2)	Bat swing speed (mph)	BEV (mph)
Original	30.732	17291	66.09	92.75
Barrel + 10%	30.732	17700	65.60	93.40
Barrel - 10%	30.732	16872	66.60	92.48
Handle + 10%	30.732	16743	66.75	92.25
Handle - 10%	30.732	17840	65.43	93.59
Barrel + 10% and Handle -10%	30.732	17775	65.50	93.76

6.5 SUMMARY

The results of the experimental measurements, finite element models and parametric studies were presented and discussed. The finite element models that were calibrated to the experimental values were used as reference and all the results of parametric studies were compared with these values. Relevant conclusions from these results are presented in the next chapter (Chapter 7).

7 CONCLUSIONS

For this research, two 33-in. long aluminum and wood bats were selected, and the respective mass, MOI, CG, COP, natural frequencies and node points on these bats were measured experimentally. The ball exit velocities and the sweet spots from these two bats were obtained by testing the bats in the BHM. It was observed that the aluminum bat outperforms the wood bat. Performance curves were drawn for these two bats, and it was observed that the sweet spot lies between the barrel node points and the COP. Finite element models of the two bats were then built and compared to experimental values using Modal Analysis for calibration purposes of these models. A ball model was built and was calibrated by adjusting the ball COR to experimental values by changing the viscoelastic material properties used for the baseball. Contact modeling between the bat and ball was then done, and the ball exit velocities and sweet spots were again calculated and compared to experimental values. Once, the velocities also compared well with the experimental values, the properties of the aluminum bat were changed to study their effect on the performance. The MOI was changed, and it was observed that barrel-loaded bat performs better than the knob-loaded bat because of the presence of more mass in the vicinity of contact. Stiffness of the bat was also changed by altering the Young's modulus, and it was observed that as the stiffness increases that the contact time between the bat and ball decreased, the hoop frequency increased and ball deformation increased. Therefore, less energy was imparted to the ball, and hence, the performance decreased

with increase in stiffness. The performance also decreased with increase in wall thickness. It was observed that frequencies increase with increase in wall thickness and hoop frequencies are sensitive to change in thickness of the barrel. It was also observed that the performance dropped with increase in hoop frequency because of the trampoline effect. It was also observed that tuning the period of oscillation of the bending frequency of the bat to the contact time will give better performance than at other frequencies. The period of oscillation was altered by changing the natural frequencies.

It was observed that the performance of an aluminum bat depends on its inertial and vibrational properties. Performance can be altered by changing either the mass distribution i.e. changing MOI or the vibrational properties. Frequency tuning of the bat, i.e. tuning the period of oscillation and changing wall thickness, will also change performance. Hoop frequencies were also observed to change the performance of the bat. Therefore, depending on the results desired, the performance of an aluminum bat can be changed to some extent by changing any of these properties. However, the attempts to tune the bat may not yield 100% results as changing one parameter may change another which might compromise the desired result.

8 RECOMMENDATIONS

There are four recommendations for future work. The first recommendation is to study the contribution of each mode of the bat during contact. The scope of this research involved studying only the effect of fundamental bending frequencies (first two) and the fundamental hoop frequencies (first one). Efforts to understand the role of other modes may yield more interesting results. The second recommendation would be to study the performance pattern of a composite bat. The research pattern followed here can be extended to a composite bat, and the composite performance can be compared with aluminum and wood bats. Also, because composite bats are anisotropic, the hoop frequencies and bending frequencies can be isolated from each other which will enable a more intensive and independent study of each of these modes. The third recommendation would be for a better ball model which may involve the layers of yarn and cork which will enable a more accurate modeling of the ball damping than was available in this study. Using linear regression analysis to conclude the locations of the nodes and the sweet spot is a fourth recommendation. Regression analysis will provide more precise results than the experimental results reported in this research.

9 LITERATURE CITED

1. http://www.amateurbaseballtoday.com/news/article_120102.php
2. Crisco, J.J. (1997) NCAA *Research Program on Bat and Ball performance*
3. Adair R.K. (1994) The Physics of Baseball, Harper-Collins, New York.
4. Nathan A.M. (2000) *Dynamics of the baseball-bat collision.* American Journal of Physics, 68(11). Pp.979-990.
5. Noble L. (1998) *Inertial and Vibrational Characteristics of Softball and Baseball Bats: Research and Design Implication*. 16th Symposium of the International Society of Biomechanics in Sports Vol. II, pp. 86-97.
6. Altair® Hyperworks®, version 6.0, product of Altair® Engineering, copy righted 1990-2003
7. LS-DYNA©, 1998-2001, version# 960, product of Livermore software technology corporation(LSTC)
8. www.thesportjournal.org/2001Journal/ summer/hard-bats.htm, 1998-2003.
9. *Physics of Sport*, (Ginn and Company, 1980), part of the Individualized Science Instructional System for Grades 9-12, developed by Florida State University.
10. Nathan A.M. (2003) *Characterizing the performance of baseball bats*. American Journal of Physics, 71(2). Pp.134-143.
11. Nathan, A.M, 'Baseball and Bat Performance Standards', talk at NCAA Research Committee meeting, OMAHA, NE, June 13, 2001.
12. R. Cross, *The sweet spot of a baseball bat,* American Journal of Physics, 66(9), 771-779 (1998).
13. Noble L., Eck, J. (1986). *Effects of selected softball Bat Loading strategies on impact reaction Impulse*. Medicine and Science in Sports and Exercise 18, 50-59.
14. Weyrich, A.S., Messier, S.P., Ruhmann, B.S., Berry, M.J. (1989).*Effects of Bat Composition, Grip Firmness, and Impact Location on Post impact Ball Velocity*. Medicine and Science in Sports and Exercise 21,199-205.

15. Brody, H. (1986). *The Sweet spot of a Baseball Bat*, American Journal of Physics 54, 640-643.
16. H. Brody, *Models of Baseball Bats*, American Journal of Physics, 58(8), 756-758 (1990).
17. Van Zandt (1991) *The Dynamical Theory of Baseball Bat*. American Journal of Physics 60. pp.72.
18. http://www.sgma.com/sports_development/bbsb/2003/techpapers/russell-tuned-bat.ppt
19. Alan. Nathan, The Physics of Baseball (or Just How Did McGwire Hit 70?) Public Lecture Parkland Community College February 9, 1999.
20. Shenoy M.M., Smith L.V., Axtell.J.T, (2001) *Performance assessment of wood, metal and composite baseball bats*. Composite Structures 52 pp. 397-404.
21. Sherwood J.A, Mustone, T.J., and Fallon, L.P. (2000) *Characterizing the Performance of Baseball Bats using Experimental and Finite Element Methods*, 3rd International Conference on the Engineering of Sport, June, Sydney, Australia.
22. ASTM standard-F1881-98 Standard Test Method for Measuring Baseball Bat Performance Factor
23. http://m-5.eng.uml.edu/ ncaa_certified_bats/NCAA_Certification% 20Protocol_27Sept1999.pdf